Politecnico di Torino

Master Degree in Ingegneria dei Materiali per l'Industria 4.0

Nanostructuring of biobased DGEVA epoxy systems by PEO-PPO-PEO triblock copolymer

Supervisors:

Prof. Marco Sangermano

Prof. Galder Kortaberria Altzerreka

Candidate:

Gianfranco Muggiolu

Academic Year 2024/2025

. Contents

. List of Figures

. List of Tables

1. Introduction

In the last decades the polymer industry is undergoing a significant transformation shifting from the petroleum-based raw materials to newly developed biobased alternatives. Additionally, the growing attention on sustainability in high performance industries, such as automotive and aerospace, ignited the research on the development of polymers, but especially epoxy resins, derived from renewable sources.

Every day the public opinion becomes more conscious about the impact of the plastic industry on the environment and human health, demanding more and more responsibility and commitment to reduce its impact. The traditional polymeric materials rely on the extraction, processing and transportation of fossil fuels, causing high greenhouse gas emissions and health hazards. The possibility to exploit renewable sources, such as biomass, at an industrial level is already a reality in the commodities industry. Regarding high performance materials, as the epoxy resins for industrial applications, the challenge is even harder. Biobased polymers must guarantee the same level of performance of the petroleum-based ones. Numerous studies have been conducted exploring different renewable sources of aromatic compounds, such as biomass and natural oils. Some formulations of biobased epoxy resins are already commercialized.

In addition, the regulations regarding both the carbon footprint and the health hazards of the plastic industry become every year more strict, imposing an urgent need to characterize and understand these biobased polymers in order to obtain materials suitable for scaling up to an industrial production.

This work investigate a commercially available epoxy resin from the diglycidyl ether of vanillin alcohol (DGEVA), cured with a petroleum-based curing agent. In particular, the main objective is the nanostructuring of the resin through the addition of a triblock copolymer, poly(ethylene oxide-b-propylene oxide-b-ethylene oxide) (PEO-PPO-PEO). Various amounts of PEO-PPO-PEO were studied from 10 to 40 wt%. The morphology of the systems was investigated and its influence on properties such as gel content, thermal stability, flexural modulus and hydrophilicity, was studied.

In addition, a preliminary study on the synthesis of dihydroxyaminopropane of vanillyl alcohol (DHAVA) from DGEVA was carried out. Through an easy and clean method the epoxy rings are substituted with amine moieties. The modified resin could represent a suitable biobased curing agent for fully biobased epoxy resin systems.

2. State of art

2.1 Epoxy resins

Epoxy resins are one of the most important types of thermosetting polymeric materials. They represent almost the 70% of the thermosets market[1], being worth \$7.2 billion in 2018[2]. This class of thermosets was discovered by the Russian chemist Prileschajew in 1909, but it was only in 1947 that the first epoxy resin was made commercially available by *Devoe-Raynolds Company*[3].

An epoxy resin is defined as a molecule characterized by the presence of more than one oxirane, or epoxide, groups[4]. The epoxides are formed by an oxygen atom which is bonded to two adjacent carbon atoms in a three membered ring group. The oxirane ring is readily opened in the presence of nucleophiles such as alkoxides, hydroxides, primary and secondary amines, etc.[5]. This family of polymers is the standard option in a wide variety of applications such as coatings, semiconductor encapsulants, printed circuit boards, adhesives, etc. This is due to their outstanding properties, such as their strength, adhesive, thermal, and electrical resistance properties[6]. The success of these resins is a consequence of their excellent resistance to chemicals, corrosion and moisture, along their high mechanical properties.

2.1.1 Petroleum based epoxy resins

Epoxy resins based on Bisphenol-A

The most widely used epoxy resin is based on the diglycidyl ether of bisphenol A (DGEBA), which represents over the 90% of the market, making it the standard for this important industrial segment[1]. DGEBA is the product of the reaction between bisphenol-A, BPA, and epichlorohydrin, ECH, in the presence of a basic catalyst. The synthesis of this resin is shown in Figure 2.1. The glycidyl ether is the most reactive epoxy function compared to terminal epoxides or epoxy groups in the middle of the carbon chain. This confers to the DGEBA a lower temperature and/or crosslinking time with respect to other types of epoxy resins. In addition, the aromatic nature of BPA leads to better thermal behaviour for this material.

The chemical structure of BPA, shown in Figure 2.1, is based on two phenols attached in the *para* position to a carbon with two methyl groups, being a rigid and highly reactive structure. However, BPA has also been classified as reprotoxic 1B by the ECHA (European Chemicals Agency) and, since march 2018, its use has been restricted for products intended for consumers[1].

Commercial DGEBA usually presents n values between 0.03 and 10; At room temperature, DGEBA is a crystalline solid for values of n close to 0, a liquid up to 0.5 and a glassy solid for $n > 0.5$.

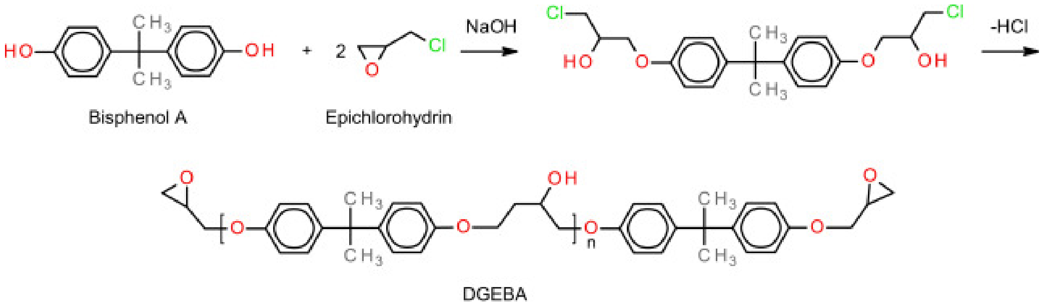

Figure 2.1: Synthesis of epoxy resin from bisphenol A and epichlorohydrin[2]

Epoxy novolac resins

Novolacs are phenol-formaldehyde condensates which can be epoxidized in order to obtain multifunctional epoxy resins. This multifunctionality guarantees excellent thermal, chemical and solvent-resistance properties thanks to their higher crosslinking density[4]. Novolac resins can also be synthesized through the reaction of bisphenol A with formaldehyde without the presence of a catalyst[7]. The chemical structure of novolac epoxy resin is shown in Figure 2.2, in which the multiple epoxy moieties along the molecule can be seen.

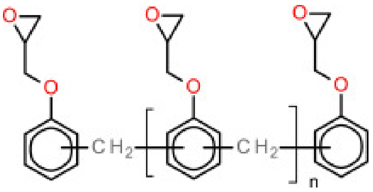

Figure 2.2: Chemical structure of novolac epoxy resins.[8]

Cycloaliphatic epoxy resins

This family of epoxy resins is represented by unsaturated compounds which present an aliphatic backbone that can be epoxidized by reacting with hydrogen peroxide or peracetic acid. Among them, the most employed one is the cycloaliphatic epoxy resin (CAE) (3',4'-epoxycyclohexyl-methyl 3,4-epoxycyclohexanecarboxylate) obtained through the reaction between 3'-cyclohexenylmethyl 3-cyclohexenecarboxylate and peracetic acid. The chemical structure of this epoxy is shown in Figure 2.3. The aliphatic backbone confers to these compounds better UV stability, a good thermal stability ad excellent electrical properties[8].

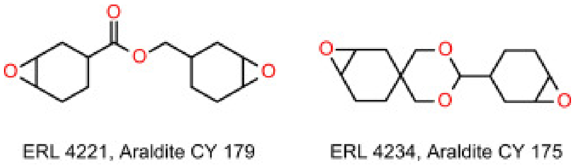

Figure 2.3: Chemical structure of cycloaliphatic epoxy resins[8]

2.1.2 Bio-based epoxy resins

As already mentioned, the on-going trend to investigate renewable alternatives to petroleum derived materials has catalized the research of both bio-based epoxy monomers and biobased curing agents. Vegetable oils, tannins and lignocellulosic biomass have already been successfully exploited as alternatives to petroleum based epoxies[9]. These biobased thermosetting materials have shown thermomechanical properties comparable to the petroleum based epoxies.

Despite being more sustainable and achieving good structural properties, they are not still competitive in an already established market, widely monopolized by the petroleum based products[10]. This is the main reason for the research to be nowadays addressed to investigate and exploit intrinsic functional properties that can be found in the bio-based materials.

Zhang et al.[11] divided the bio-based epoxy resins into two categories: the partly bio-based epoxy thermosets, containing biobased epoxy monomer or biobased curing agent, and fully biobased thermosets, containing both bio-based epoxy monomer and biobased curing agent.

Bio-sourced DGEBA

The first approach for the synthesis of bio-based epoxy resins could be looking for pathways to synthesize DGEBA, the most used resin, trough alternative bio-sourced reagents. As already mentioned, DGEBA is obtained through the reaction of BPA and ECH. The latter is already commercialized in a biobased form obtained from glycerol. Using biobased ECH leads to DGEBA with up to 28% of carbon content from biomass. This percentage can increase up to 56% if BPA is partially synthesized from phenol and biobased acetone[1].

In this case, the biobased resin shows the same properties of a petroleum-sourced DGEBA, as the chemical structure is the same. On the other hand, sharing the identical chemical structure leads to the same toxicity problems of the already used DGEBA. Other biobased molecules must be studied in order to obtain a resin with comparable properties to those of DGEBA, while allowing to use fewer toxic reagents.

Cardanol-based epoxy resins

Cardanol is a lipid which can be extracted from cashew nutshell oil (Cashew NutShell Liquid or CNSL), one of the largest renewable natural sources of phenolic compounds. Cardanol is a mixture of meta-alkylphenols presenting different degrees of unsaturation. The phenolic hydroxyl function can be easily functionalized by direct reaction with ECH, leading to a highly reactive phenolic glydicyl ether function. Through a two-step reaction is possible to obtain a di-glycidyl cardanol which can be exploited as an epoxy resin monomer. This compound is also marketed by Cardolite® Corporation under the name NC-514[1]. The chemical structure of this resin is depicted in Figure 2.4.

CNSL presents a limited availability, around 125000 tons per year; such limited volume is not sufficient to consider CNSL as a reliable resource and could represent a drawback for cardanol use as a DGEBA substitute[12].

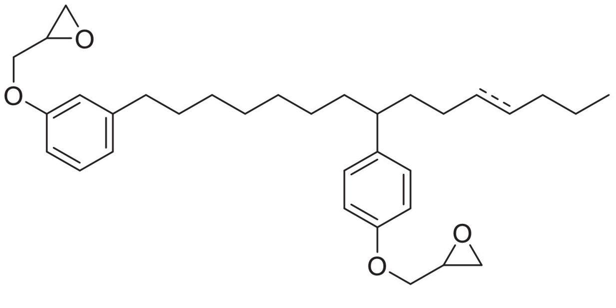

Figure 2.4: Chemical structure of diglycidyl cardanol (Cardolite®NC-514)[1]

.

Lignin derived epoxy resins

Lignin is the most abundant bio-derived source of aromatic compounds[13], containing about 30% of non-fossil organic carbon on Earth[14]. The volume of commercially available lignin is around 1 million tons per year, even if it presents a much higher potential[12]. The building blocks of lignin are three aromatic alcohols, called monolignols: guaiacyl (G-type lignin), syringyl (S-type lignin) and p-hydroxyphenyl (H-type lignin). The structural units derived from the polymerization of these alcohols are referred to as phenylpropane units[15].

Nowadays, one of the most promising ways to exploit the aromatic nature of lignin is the depolymerization of the macromolecule in order to obtain lignin-derived aromatic compounds with lower molecular weight and, consequently, higher reactivity. In particular, two phenol derivates of lignin that have been extensively studied as epoxy resins monomer precursors, are the eugenol and the vanillin[15].

Eugenol-based epoxy resins Eugenol is a natural phenol that can be easily extracted from the lignin molecule. It presents a phenylpropanoid structure, as seen in Figure 2.5. The phenolic hydroxyl and the terminal olefin are highly reactive moieties that can be exploited in the epoxidation of the eugenol[16].

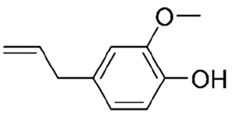

Figure 2.5: Chemical structure of eugenol[16]

In order to obtain an epoxy monomer from an eugenol molecule, the simplest way is a diepoxidation, through which a 2-[3-methoxy-4-(oxirane-2-ylmethoxy)benzyl]oxirane can be obtained. *Qin et al.*[17] have successfully synthesized this compound in a three-step process, as shown in Figure 2.6. The resulting molecule presents two epoxy moieties making it a suitable candidate for epoxy resins.

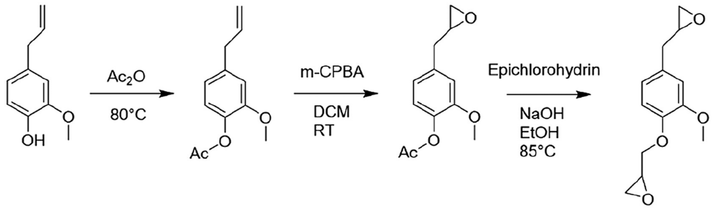

Figure 2.6: Synthesis of 2-[3-methoxy-4-(oxirane-2-ylmethoxy)benzyl]oxirane[16]

Taking into consideration the chemical structure od DGEBA another pathway to exploit eugenol is the synthesis of a diglycidyl ether. *Zhao et al.*[18] used 2-methoxy-4-propylphenol (dihydroeugenol) to synthesize a diglycidylether of dihydroeugenol, throught the process shown in Figure 2.7. The epoxy resin obtained presented comparable properties to the petroleum-based ones.

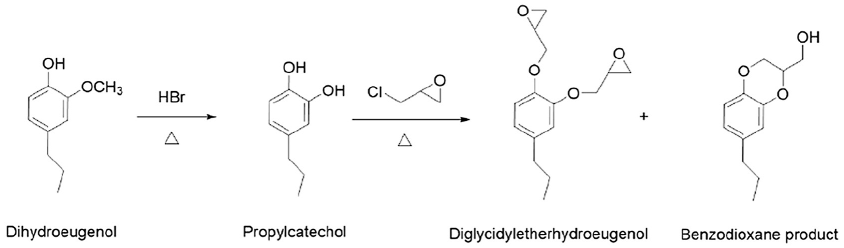

Figure 2.7: Synthesis of diglycidylether of dihydroeugenol[18]

Vanillin-based epoxy resins Vanillin is a natural molecule and contains both phenolic hydroxyl and aldehyde groups, which can both be easily functionalized with epoxy functions[11]. Each year around 20.000 tons of vanillin are produced, the 15% of which is extracted from lignin[12]. The easiest pathway to obtain an epoxy monomer from vanillin is to convert this molecule into vanillic acid, vanillic alcohol and 2- methoxyhydroquinone, which are three different molecules, depicted in Figure 2.8, that can produce diepoxidized glycidyl ether functions through direct reaction with ECH[1].

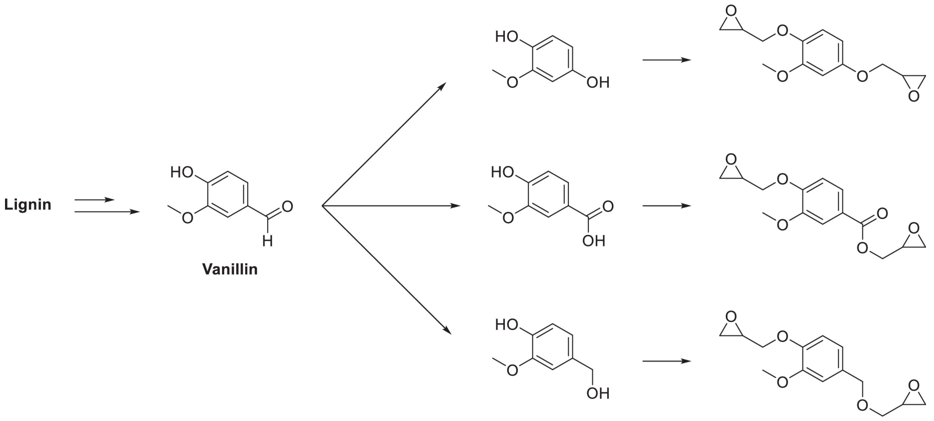

Figure 2.8: Synthesis of epoxidized vanillin derivatives from lignin[1]

2.2 Curing agents

Almost all epoxy systems are transformed into infusible and insoluble thermoset networks with great mechanical and thermal properties by curing with crosslinkers or hardeners. The final properties of an epoxy resin highly depends on the curing agent used in their formulation; they affect not only the viscosity and reactivity, but also determine the crosslinking degree and the nature of the chemical bonds formed during the curing process[4]. The crosslinking reaction in epoxy resins usually involves the epoxy moieties, but it can also take place in the hydroxyl functions along the chain. Reaction with the epoxy function consists in the opening of the oxirane ring and the formation of linear C-O bonds, leading to a bridge between the macromolecules with low shrinkage and improved mechanical properties.

The most common hardeners in epoxy resins are coreactive, acting as a comonomer in the polymerization process[4]. The epoxy moiety can react with both electrophilic and nucleophilic compounds; the curing agents can be divided into two major classes, as a function of the mechanism: alkaline and acidic[2].

Aliphatic amines

Primary and secondary aliphatic amines are the widest used alkaline curing agents for epoxy resin manufacturing. The path of reaction of these curing agents is shown in Figure 2.9. A primary amine function reacts with the oxirane ring, forming a compound presenting an hydroxyl group and a secondary amine. The secondary amine can subsequently react once again to form another hydroxyl and a tertiary amine, leading to a higher crosslinked structure. Aliphatic amines are highly reactive compounds used in fast curing epoxies at room temperature. The most common hardeners belonging to this family are diethylene triamine (DETA), tetraethylene pentaamine and triethylenetetramine (TETA)[2].

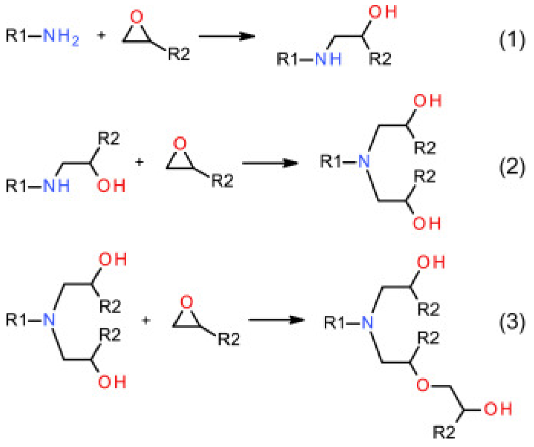

Figure 2.9: Reaction mechanism between amines and oxirane rings[2]

Aromatic amines

The crosslinking mechanism is the same than that for the aliphatic amines, but the presence of the aromatic rings in the structure allows to obtain an epoxy resin with higher thermal stability and mechanical properties. Nonetheless, the aromatic nature of these compounds reduces their reactivity; resins cannot be cured at room temperature, but they require heat in order to react. This feature increases the pot-life of the systems, but it also increases their cost. The most common aromatic amines used as curing agents are 4-4'-diaminophenyl sulphone (DDS) and m-phenylenediamine (MPDA)[2]. Their chemical structure is depicted in Figure 2.10.

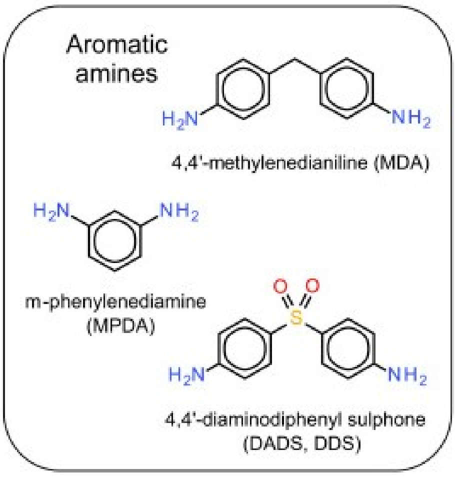

Figure 2.10: Chemical structure of aromatic amines[2]

Cyclic anhydrides

The cyclic anhydrides are the most used acid curing agents for epoxy resins. For these compounds the oxirane ring opening reaction is often caused by the presence of water or hydroxyl groups. The mechanism is shown in Figure 2.11. The simplest cyclic anhydride is the phtalic anhydride (PA), but some other commonly used molecules are nadic methyl anhydride (NMA) and pyromellitic dianhydride (PMDA). Their structures, along some other common cyclic anhydrides, are shown in Figure 2.12.

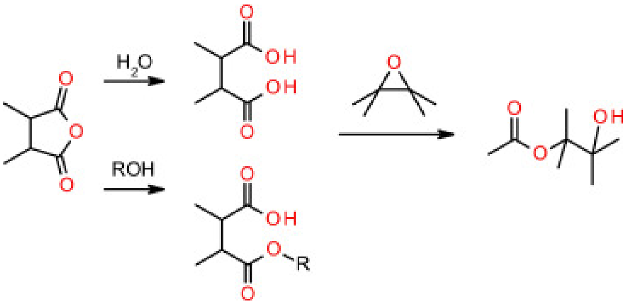

Figure 2.11: Reaction mechanism between cyclic anhydrides and oxirane rings[2]

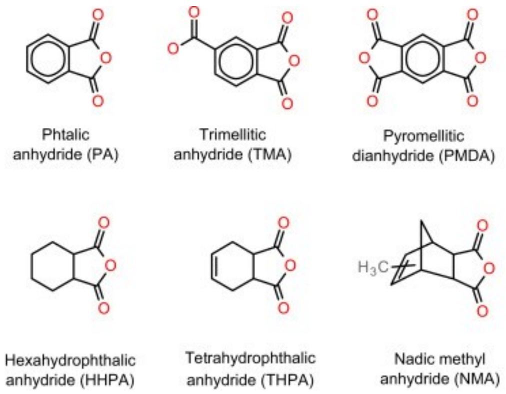

Figure 2.12: Chemical structure of cyclic anhydrides[2]

2.2.1 Bio-based curing agents

Commonly used hardeners, as those above mentioned, are molecules deriving from petrochemical resources, which have been proven to be the cause of environmental and health hazards[11]. In the last two decades, along the research regarding the epoxy monomers, scientists developed methods to also synthesize curing agents from biomass and other biobased raw materials.

Bio-based curatives containing amines

Vanillin, limonene and eugenol are just a few biomass derived chemicals that have been exploited successfully to obtain curing agents. The diamine of methylated divanillylamine (MDVA), the synthetic diamines of aromatic diamine-allyl eugenol (DA-AE) and cyclic diamine-limonene (DA-LIM) have all been reported as hardeners for epoxy thermosets[11]. Their chemical structures and synthesis procedures are shown in Figure 2.13 and Figure 2.14, respectively.

Bio-based curatives containing acid anhydride

Cardanol has been successfully modified in order to obtain two different compounds (Car-DCP-MAH and Car-DPC-MAH) as alternatives for the petroleum-based 4,4’-diaminodiphenylmethane (DDM). The synthesis of these compounds is shown in Figure 2.15.

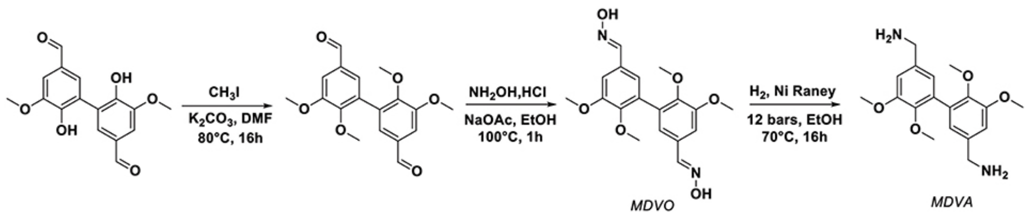

Figure 2.13: Synthesis of methylated divanillylamine from divanillin[19]

2.3 Block copolymers

Block copolymers (BCPs) are a class of heterogeneous polymers consisting in two or more homopolymers which coexist in a single macromolecule. BCPs can self-assemble presenting spontaneous spatial organization at the nanoscale: the blocks are thermodynamically incompatible but they cannot macro-separate as they are covalently bonded, so they led to a micro or nanophase-separation, leading to an array of periodic nanostructures which are often referred to as micro or nanophase-separated structures[22].

A great variety of micro or nanoseparated structures can be obtained depending on many factors such as block nature and ratio, molar mass, solvent employed, annealing procedure if any, temperature, etc. This self-assembly phenomenon offers plenty of potential applications in nanotechnology and new materials. Among them, the nanostructuring of thermosetting matrices should be mentioned.

BCPs have been deeply studied as toughening agents in thermosetting polymers. In fact, one of the main drawbacks of thermosetting resins is their low fracture toughness. BCPs offer a double improvement: an increased fracture toughness and the possibility to obtain a nanostructured polymer, which can be exploited as template for selective localization of organic or inorganic nano-entities[23].

2.3.1 Block copolymers self-assembly

The microphase-separated structures obtained through this segregation of the different blocks on the molecular scale (5-100 nm) lead to different complex morphologies. These structures are intrinsically driven by several parameters such as Flory-Huggins interaction parameter among the blocks (χ), degree of polymerization (N) and volume fraction (f)[24].

In the manufacturing of nanostructured resins the morphologies can be adjusted by changing f, while keeping χN (segregation product[22]) constant. In Figure 2.16 the equilibrium morphologies which can be obtained for a diblock copolymer are shown as an example: spheres, hexagonally packed cylinders,gyroid and lamellae.

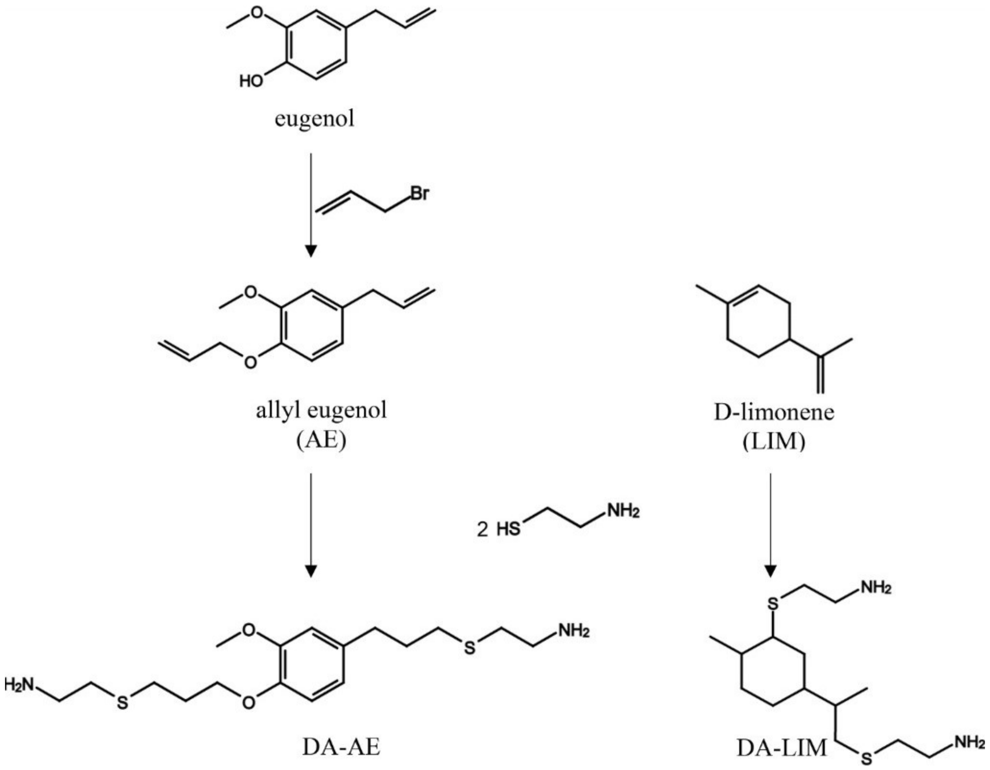

Figure 2.14: Synthesis of the diamines DA-AE and DA-LIM[20]

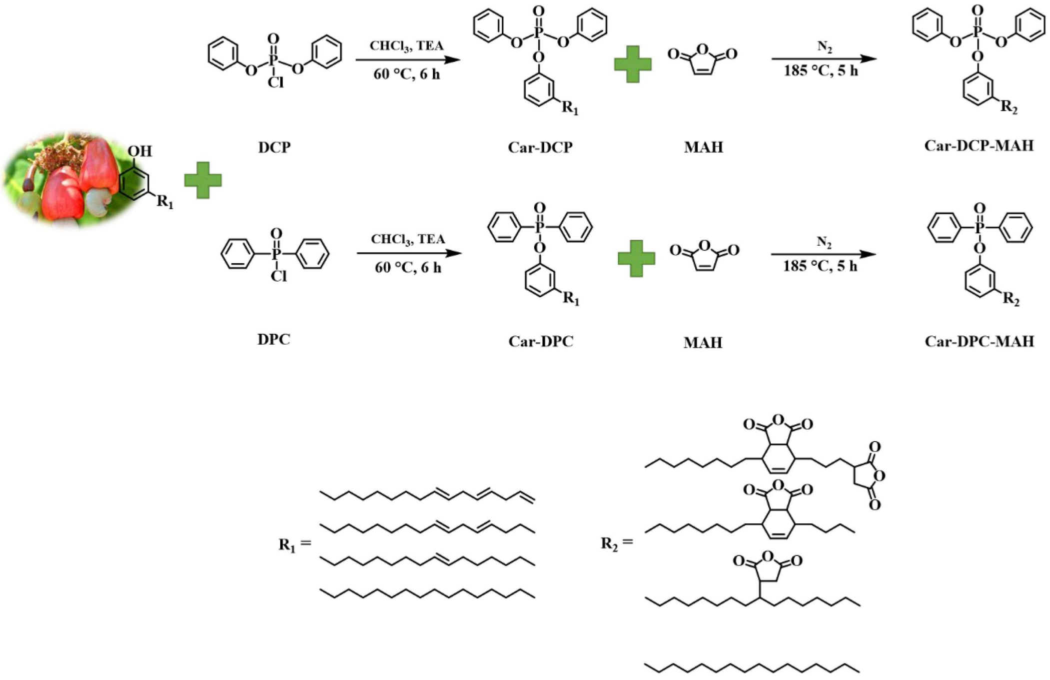

Figure 2.15: Synthesis of Car-DCP-MAH and Car-DPC-MAH[21]

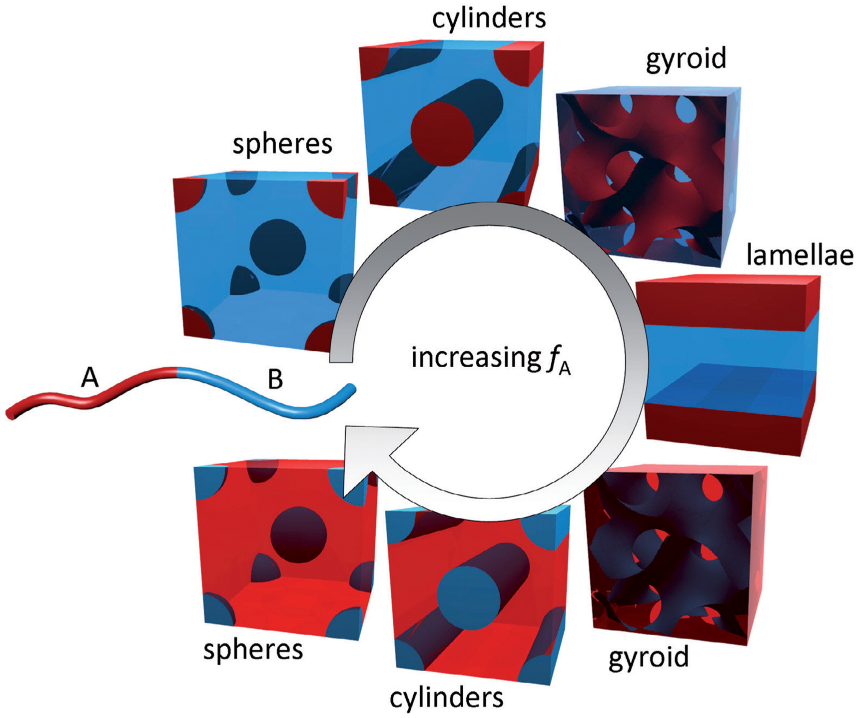

Figure 2.16: BCPs morphologies with increasing volume fraction[25]

2.3.2 Nanostructured epoxy resins

As already mentioned, BCPs have been deeply studied as toughening agents for thermosetting polymers, especially epoxy resins. In addition, they have proven to be perfect candidates for obtaining templates at the nanoscale. There are two distinct pathways for nanostructuring epoxy resins[23]: the employment of amphiphilic BCPs or the chemical modification of one of the blocks.

Amphiphilic BCPs This method exploits the difference in miscibility of the blocks of the copolymer. An amphiphilic BCP usually presents an hydrophilic block, which is miscible with the epoxy, and an hydrophobic one, immiscible with the matrix;

Functionalized BCPs This method consists in chemically modifying the BCPs in order to have at least one functionalized block with improved compatibility with the epoxy matrix.

In addition, depending on the nature of the system it is possible to identify two different mechanisms of morphology formation[23]:

Initial self-assemlby The epoxy monomers act as a selective solvent of at least one block leading to a microphase segregation that occurs before the curing reaction. In this case, the crosslinking allows to fix the final morphology but does not partecipate in the formation of the nanostructure;

Reaction induced microphase separation (RIPS) At first all the blocks of the BCP are miscible with the epoxy system and the microsegregation is induced by the network formation. In this case, the crosslinking is responsible of generating the microphase-separated structures.

3. Experimental Part

3.1 Materials

3.1.1 Epoxy resin

The epoxy resin used is a commercially available diglycidyl ether of vanillin alcohol (DGEVA), synthesized by *Specific Polymers*, Castries, France. The resin has a molecular weight of 266.29 g/mol and has an epoxide equivalent of 133-148 g/mol. At room temperature DGEVA is a white wax. The chemical structure is shown in Figure 3.1.

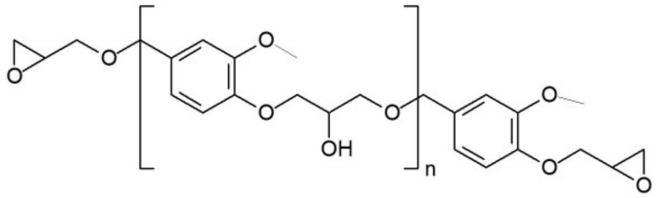

Figure 3.1: Chemical structure of vanillyl alcohol diglycidyl ether

3.1.2 Curing agent

The cross-linking agent used is a commercial grade 4,4'-diaminodiphenylmethane (DDM), purchased from *Sigma-Aldrich*, Darmstadt, Germany. It is a crystalline solid with molecular weight of 198.26 g/mol. Its chemical structure is reported in Figure 3.2.

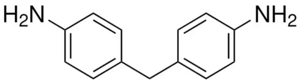

Figure 3.2: Chemical structure of 4,4'-diaminodiphenylmethane

3.1.3 Block copolymer

The block copolymer used is Pluronic F-127, a poly(ethylene oxide-b-propylene oxide-b-ethylene oxide) (PEO-PPO-PEO) triblock copolymer commercialized by *Sigma-Aldrich*, Darmstadt, Germany. It has a molecular weight of 12600 g/mol and a HLB of 18-23. Its chemical structure is shown in Figure 3.3.

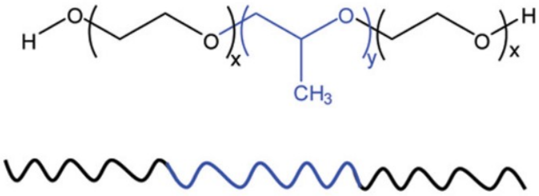

Figure 3.3: Chemical structure of PEO-PPO-PEO triblock copolymer[26]

3.2 Sample preparation

Different DGEVA/DDM epoxy systems were prepared with several amounts of PEO-PPO-PEO triblock copolymer. In particular, the systems evaluated in this report contain 10 (DGEVA/DDM-BCP10), 20 (DGEVA/DDM-BCP20) and 40 wt% (DGEVA/DDM-BCP40) of BCPs, with a neat DGEVA/DDM system (DGEVA/DDM) as reference.

3.2.1 Bulk samples

The bulk samples were prepared with the following method. First, the materials were kept under vacuum at 50°C for at least 24 h. Then, DGEVA and PEO-PPO-PEO were mixed and stirred in an oil bath at 80°C. The mixture was degassed at 60°C for 15 min. After the degassing, DDM was added in a stoichiometric amount to the mixture while stirring in the oil bath at 80°C, until a homogeneous blend was obtained. The blend was degassed at 60°C for 15 min.

After the second degassing, the DGEVA/DDM/PEO-PPO-PEO system was transferred into the mold, previously coated with an antisticking agent. The molded sample was degassed at 80°C until all the bubbles were removed. Then, it was put into the oven to cure. The samples were cured for 6 h at 120°C and post-cured for 2 h at 190°C. The curing cycle was identified in a previous work[27].

3.2.2 Dihydroxyaminopropane of vanillyl alcohol synthesis

The synthesis of the biobased curing agent, dihydroxyaminopropane of vanillyl alcohol (DHAVA), was achieved through the amination of DGEVA, through the following method. In a flask, 1 g of DGEVA was added in 4,8 mL of 1,4-dioxane and stirred at 110°C until completely solved. After, $NH_3 \cdot H_2O$ (25% solution, 4.8 mL) was added. The system was left at 110°C, continuously stirring. The synthesis was carried out for 3 h. A rotatory evaporator was then used to remove the solvent and residual $NH_3 \cdot H_2O$.

3.3 Techniques

Differential scanning calorimetry (DSC) Dynamic DSC measurements were performed to investigate the thermal behaviour of DGEVA/DDM-BCP systems. The scans were performed from -80°C to 250°C at 10°C/min scan rate. Prior to this scan, a heating from -80°C to 250°C followed by a cooling from 250°C to -80°C was carried out to delete the thermal history of the material. All tests were performed under nitrogen atmosphere, with a flow of 10 mL/min. The T_g of the samples was calculated as the onset of the step. In addition, the theoretical $T_{g,TH}$ of the DGEVA/DDM-BCP systems was calculated using the Fox equation[28]:

$$\frac{1}{T_{g,TH}} = \frac{w_{BCP}}{T_{g,BCP}} + \frac{w_{DGEVA/DDM}}{T_{g,DGEVA/DDM}}$$

Thermogravimetric Analysis (TGA) Thermogravimetric tests were performed on a TGA 500 from TA Instruments Inc. (New Castle, DE, USA). Samples were heated from 25 to 800 °C with a heating rate of 10 °C/min under nitrogen atmosphere.

Fourier-Transformed Infrared Spectroscopy (FTIR) FTIR spectra were acquired with a Nicolet Nexus spectrometer from Thermo Fisher Scientific SL (Bilbao, Spain), provided with a Golden Gate ATR sampling accessory. The spectra were recorded in the range of 4000-650 cm^{-1}, performing 16 scans with a resolution of 4 cm^{-1}.

Atomic Force Microscopy (AFM) AFM analysis was used to study the morphologies of the cured DGEVA/DDM-BCP systems. AFM was used under ambient condition, using a scanning probe microscope Multimode 8 from Bruker (Billerica, MI, USA). Tapping mode (TM) was employed in air, using an integrated tip (125 mm in length with a 300 kHz resonant frequency). Measurements were carried out with 512 scan lines and target amplitude around 0.9 V. Bulk samples were cut using an ultramicrotome Leica Ultracut R provided with a diamond blade.

Contact Angle measurement Water contact angle measurements were recorded using Data Physics OCA 20 contact angle system at ambient temperature. Before being tested, the surface of the samples was cleaned with acetone and left to dry in vacuum at 40 °C for at least 48 h. 5μL distilled water drop was used for each measurement. At least five measurements were carried out for each system. In addition, the surface free energies of the systems were calculated using the Berthelot's rule[28]:

$$\gamma_{SV} = \frac{(1 + \cos\theta)^2}{4}\gamma_{LV}$$

Three-Point Flexural tests The mechanical behaviour of the cured systems was determined using a universal testing machine (Instron, 5967), provided with a 30 kN load cell. Three-point flexural tests without notch were performed. The samples were parallelepipedal bars of 30 x 6 x 1.5 mm^3. The crosshead rate was 1 mm min^{-1}. Flexural modulus was determined as the slope of the load-displacement curve in the zone of linear elasticity. Five measurements were carried out for each system and the average was taken as final value.

Swelling Index and Gel Content tests The swelling index (SI) and the gel content (GC) were measured for all the systems. 60 mg samples were cut and cleaned with acetone and left to dry at 40°C in vacuum for at least 24 h. The initial mass of the cleaned sample (m_0) was measured, then they were put in 10 mL of THF for 24 h, while continuously stirring. After, the samples were removed from the solvent and the mass was measured again (m_1). Finally, the samples were dried in a vacuum oven at 70 °C for 24h. The final mass (m_2) was recorded.

The swelling index was calculated using the following equation[29]:

$$SI = \frac{m_1 - m_0}{m_0} * 100$$

The gel content was measured using the following expression[30]:

$$GC = \frac{m_2}{m_0} * 100$$

^{1}H - Nuclear Magnetic Resonance (^{1}H-NMR) ^{1}H-NMR was used to determine the chemical structure of the modified resin. The analysis was carried out using a RMN Bruker Avance Neo 500 spectrometer, with a resonance frequency of 500 MHz. The samples were kept at 25 °C during the measurements.

4. Results

4.1 Bulk samples

4.1.1 Differential Scanning Calorimetry Analysis (DSC)

Dynamic DSC analysis was performed on all DGEVA/DDM-BCP cured bulk systems. The obtained thermograms are shown in Figure 4.1. The DGEVA/DDM system presents a T_g at 112.2°C. For the systems with PEO-PPO-PEO triblock copolymer the T_g decreased continuously with the BCP content, varying from 95.9°C for the DGEVA/DDM-BCP10 blend to 76.7°C for the DGEVA/DDM-BCP40 one. This trend confirms the miscibility between DGEVA resin and the PEO block of PEO-PPO-PEO.

The system DGEVA/DDM-BCP40 differs from the others by showing three distinct glass transition temperatures. The first T_g is recorded at -72.3°C and could be attributed to a phase of neat PEO-PPO-PEO triblock copolymer expelled out during the epoxy-amine curing reaction. A second T_g appears at -62.9°C, this could be referred to a PEO phase with DGEVA. The third T_g appears at 76.7°C and it corresponds to a PEO-rich DGEVA phase.

In Table 4.1 the theoretical $T_{g,TH}$ is also reported. The equation revealed that with increasing amount of PEO-PPO-PEO triblock copolymer the T_g of the systems decreases proportionally. Nonetheless, the experimental glass transition temperatures are higher with respect to the theoretical values, proving of a partial miscibility of the copolymers in the epoxy matrix.

In addition, the dynamic thermograms of DGEVA/DDM-BCP systems presented endothermic peaks. The DGEVA/DDM-BCP10 system present a small peak centered at 57.2°C. With higher amounts of BCP two peaks appear, which tend to become higher and closer as the BCP content is increased. This could be justified with the presence of different types of crystals in the systems[27]. These peaks could be attributed to the melting of the PEO block of the PEO-PPO-PEO triblock copolymer, which presents a melting peak centered at 58.8°C, as shown in the thermogram of neat PEO-PPO-PEO in Figure 4.2.

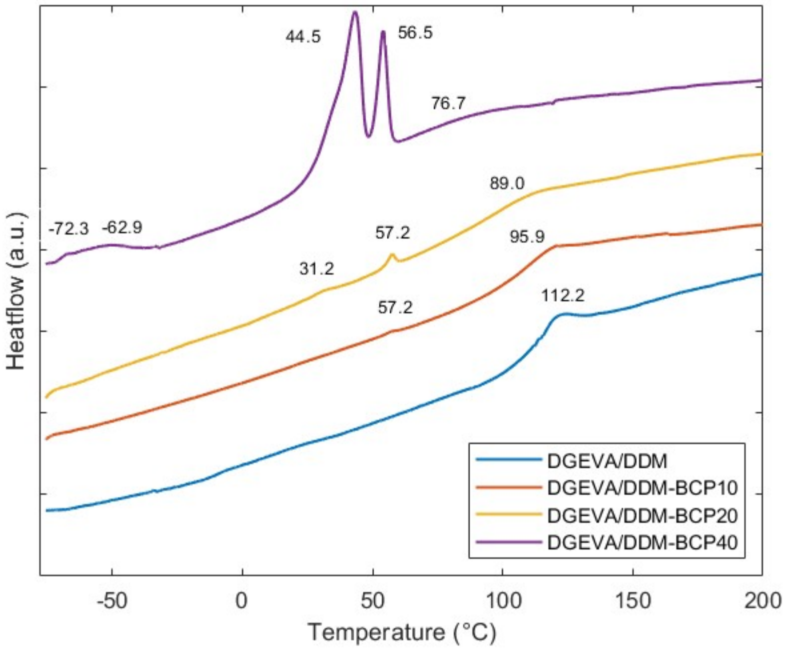

Figure 4.1: Dynamic DSC thermograms of DGEVA/DDM-BCP systems with BCP content from 0 to 40 wt%

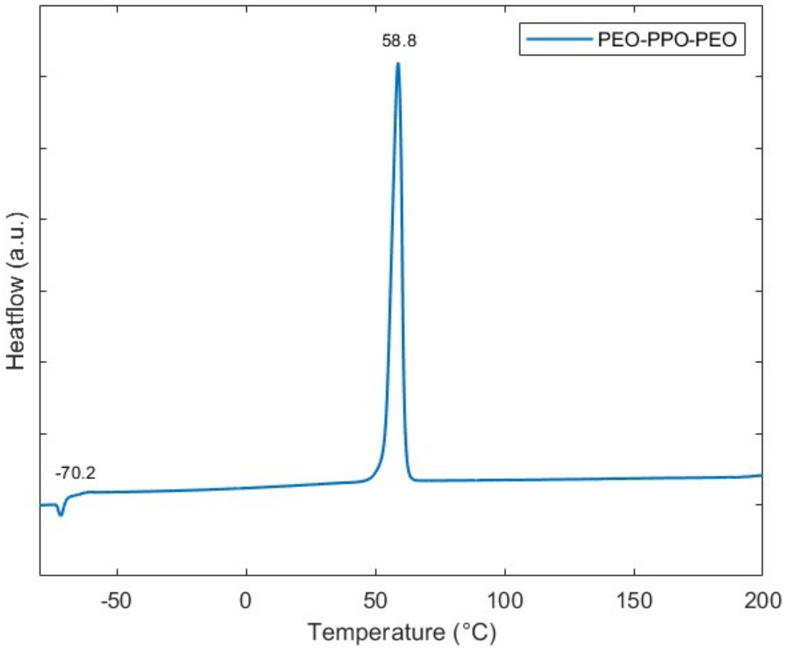

Figure 4.2: Dynamic DSC thermogram of PEO-PPO-PEO triblock copolymer

Table 4.1: Dynamic DSC results for DGEVA/DDM-BCP systems with BCP content from 0% to 40%

	T_g (°C)			T_m (°C)		$T_{g,TH}$ (°C)
DGEVA/DDM	-	-	112.2	-	-	112.2
DGEVA/DDM-BCP10	-	-	95.9	-	57.2	80.3
DGEVA/DDM-BCP20	-	-	89.0	31.2	57.5	53.4
DGEVA/DDM-BCP40	-72.3	-62.9	76.7	44.5	56.5	10.4
PEO-PPO-PEO	-70.2	-	-	-	58.8	-70.2

4.1.2 Thermogravimetric Analysis (TGA)

Thermogravimetric analysis of cured DGEVA/DDM-BCP systems were performed. The data of the analysis are reported in Table 4.2. All four systems present the onset of thermal degradation between 365-375°C, as it's possible to see in the curves in Figure 4.3. The BCP addition, and their weight fraction, do not affect the thermal stability of the epoxy system. On the other hand, the values of T_{50} decrease between the DGEVA/DDM system and the DGEVA/DDM-BCP40, from 443 to 404°C, respectively; as a result, the presence of PEO-PPO-PEO slightly anticipates the degradation of the system. The formed char amount decreases proportionally to the PEO-PPO-PEO content in the system, decreasing from 36.3% of DGEVA/DDM system to 20.6%, corresponding to the sample of DGEVA/DDM-BCP40.

In Figure 4.4 the DTG curves are reported. The maximum decomposition rate, that is the DTG peak, slightly increases with BCP content from 385°C for the DGEVA/DDM system to 403°C for the DGEVA/DDM-BCP40 one. In addition, this system presents a second smaller peak at 92°C that could be associated with higher retained humidity in the sample, caused by the higher amount of hydrophilic PEO-PPO-PEO.

Table 4.2: Results of TGA and DTG of bulk DGEVA/DDM-BCP systems

	T_{onset} (°C)	T_{50} (°C)	Residual mass (%)	DTG peak(°C)
DGEVA/DDM	366	440	36.3	385
DGEVA/DDM-BCP10	366	414	33.4	393
DGEVA/DDM-BCP20	367	408	30.4	398
DGEVA/DDM-BCP40	373	404	20.6	403

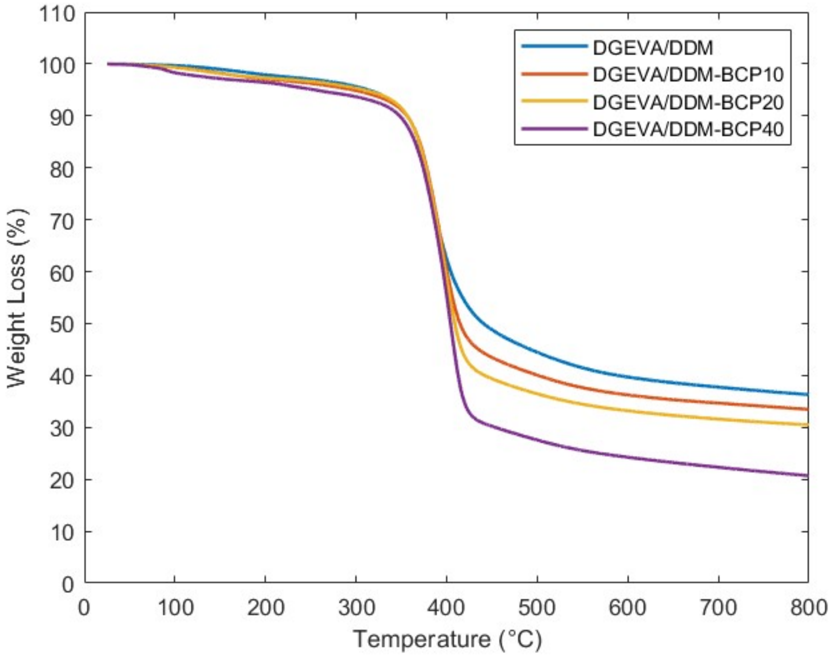

Figure 4.3: TGA curves of DGEVA/DDM-BCP systems with BCP content from 0 to 40 wt%

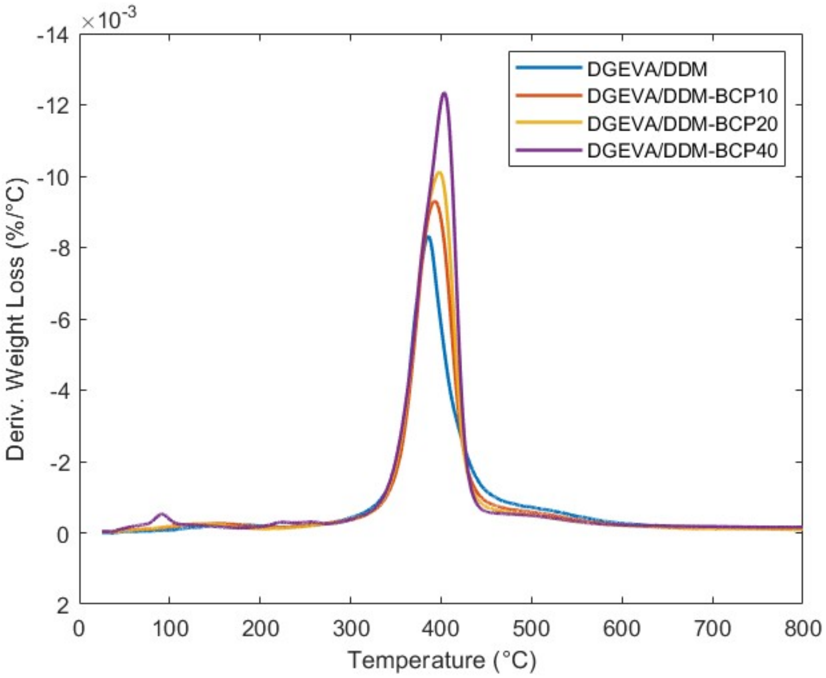

Figure 4.4: DTG curves of DGEVA/DDM-BCP systems with BCP content from 0 to 40 wt%

4.1.3 Fourier-Transform Infrared Spectroscopy (FTIR)

FTIR spectra (Figure 4.5) of pristine DGEVA resin and cured DGEVA/DDM system were recorded and analysed to study the epoxy-amine curing reaction. In the pristine DGEVA spectrum the typical peak of the epoxy rings is centered at 910 cm^{-1}(pointed by the arrow) . This peak is not present in the DGEVA/DDM spectrum, confirming a successful curing reaction with the opening of all epoxy rings. Similarly, *Noè et al.*[31] studied the curing of DGEVA epoxy systems, with a UV-activated reaction, following the intensity of the peak at 910 cm^{-1} .

In addition, the pristine DGEVA presents a broad peak centered at 3433 cm^{-1}, which can be attributed to the stretching vibration of hydroxyls present in the sample due to retained humidity. After curing this peak gains intensity and undergoes a redshift to 3380 cm^{-1}. In the DGEVA/DDM sample this peak can be attributed both to the -OH and -NH in the system. The curing reaction forms amine and hydroxyl moieties in the molecule through the opening of the oxirane rings.

In Figure 4.6 the spectra of DGEVA/DDM-BCP systems are reported. In all the cured systems the peaks related to the epoxy rings (at 910 cm^{-1}) do not appear, proving of a complete curing reaction, as mentioned above, for all the BCP content analysed. All the spectra present a broad peak centered in the region from 3380-3350 cm^{-1}, which can be attributed to the -OH and -NH stretching vibration, as mentioned above. With increasing BCP content the peaks of hydroxyls are shifted to lower frequencies, from 3380 cm^{-1}(DGEVA/DDM system) to 3367 cm^{-1} of the DGEVA/DDM.BCP40 system. This redshift could indicate that the -OH of the epoxy network undergo some stretching due to hydrogen bonding between the ether moieties of the PEO blocks of PEO-PPO-PEO triblock copolymer and the hydroxyls formed after the ring-opening reaction[32]. This redshift of -OH strecthing vibrations additionally confirms the miscibility of the PEO blocks in the DGEVA resin matrix.

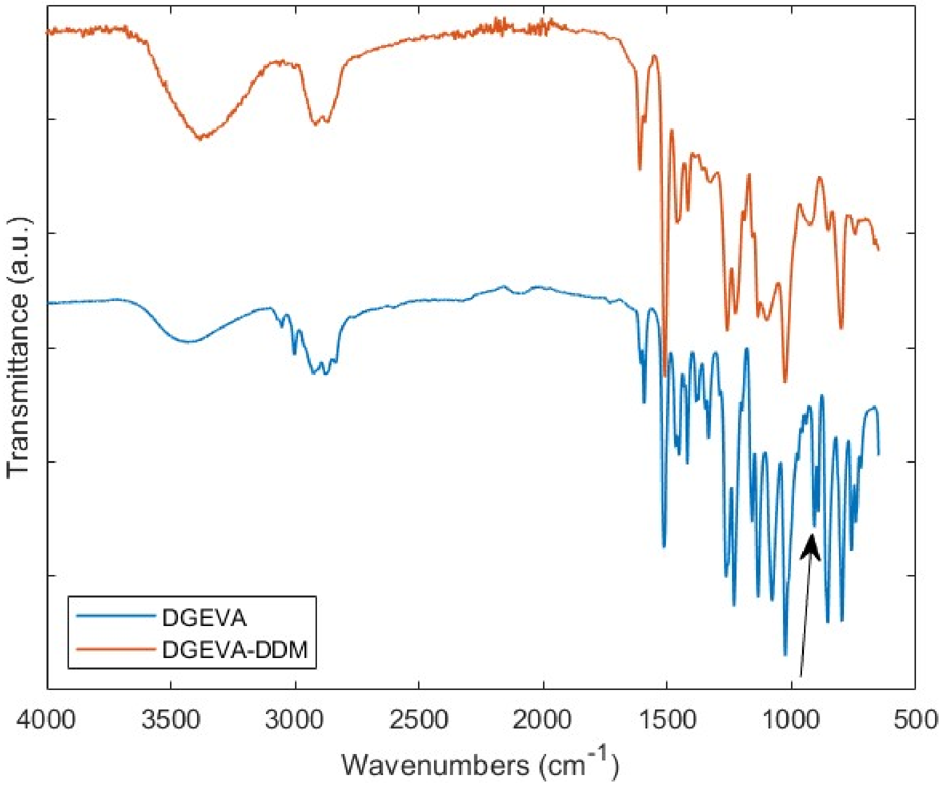

Figure 4.5: FTIR spectra of DGEVA and DGEVA/DDM cured system

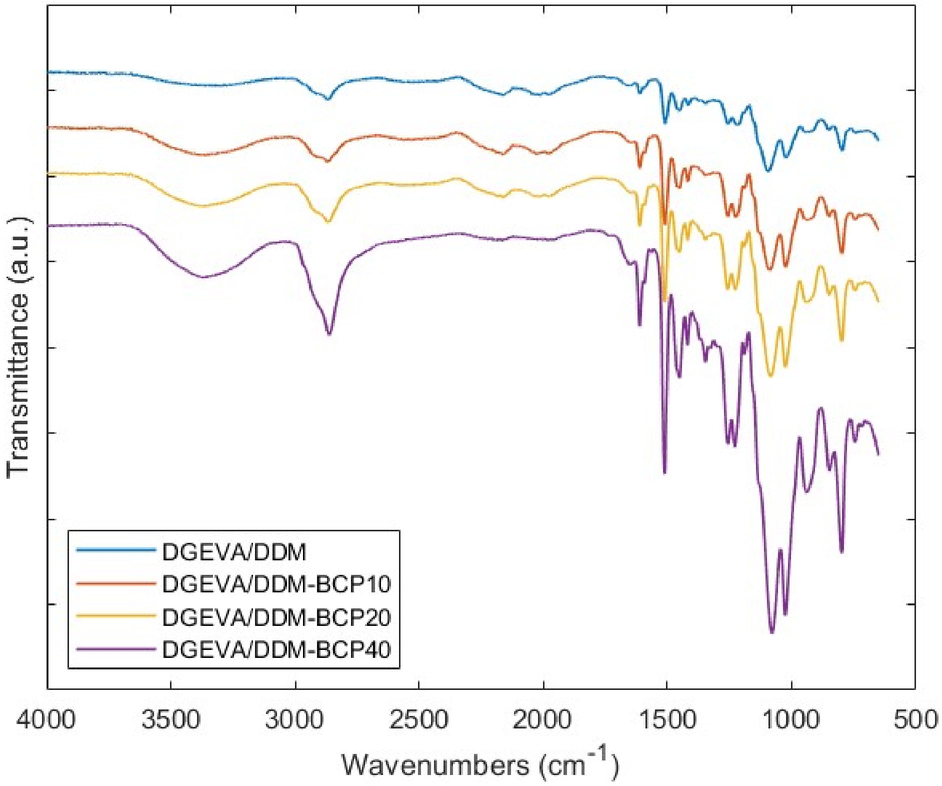

Figure 4.6: FTIR spectra of DGEVA/DDM-BCP systems with BCP content from 0 to 40 wt%

4.1.4 Atomic Force Microscopy

AFM was used to study the morphologies of DGEVA/DDM-BCP systems. The acquired phase images, with scan sizes of 3 and 1 μm, are reported in Figure 4.7 and 4.8, respectively. The complete results are reported in the supplementary material.

In Figure 4.7 it's possible to observe that the morphology of all the samples is homogeneous. The DGEVA/DDM (A), taken as the reference system, present a smooth surface related to a completed amorphous system. The systems with 10 (B) and 20 wt% (C) BCP show a higher surface roughness caused by the nanodomains related to the PPO blocks of the PEO-PPO-PEO triblock copolymer. The DGEVA/DDM-BCP40 system (D) differs from the previous ones because it presents crystalline domains.

In Figure 4.8 it's possible to analyse the different morphologies of the systems. Once again, the DGEVA/DDM one (A) is used as reference and it present itself as a completely uniform system. In the system with 10 wt% of BCP (B) a sphere-like morphology is formed: dark spherical domains with diameters ranging from 17 to 20 nm can be attributed to the PPO blocks which cannot be solved in the epoxy matrix, while the continuous light phase is the PEO-rich DGEVA/DDM phase. Increasing the BCP content up to 20 wt% (C) modifies the morphology: in this case an hexagonally packed cylinder morphology is formed, with the PPO block phase with diameters slightly smaller (14-17 nm) with respect to the DGEVA/DDM-BCP10 system, surrounded by the continuous PEO rich DGEVA phase. In the DGEVA/DDM-BCP40 system (D) it's still possible to see some spherical domains of the PPO rich phase, but the nanostructures are disrupted by the formation of crystalline regions. This is in accordance with the DSC results, in which this system presents two endothermic peaks with a higher intensity with respect to the other systems.

The AFM characterization confirms the nanostructuring of the DGEVA/DDM-BCP systems. The PEO blocks of the triblock PEO-PPO-PEO copolymer solve into the DGEVA matrix thanks to the hydrogen bonding between the ether group of PEO and the hydroxyls of the epoxy resin, meanwhile the PPO blocks are immiscible in the system and self assemble into nanodomains, which are set during the epoxy-amine curing reaction of the DGEVA/DDM. With higher amount of BCP a portion of the PEO is also expelled out from the DGEVA during the curing cycle. The PEO which is not mixed with the epoxy forms the crystalline regions as discussed for the DGEVA/DDM-BCP40 system. *Parameswaranpillai et al.*[33] reported a similar behaviour of the PEO-PPO-PEO triblock copolymer in a DGEBA epoxy resin cured with DDM.

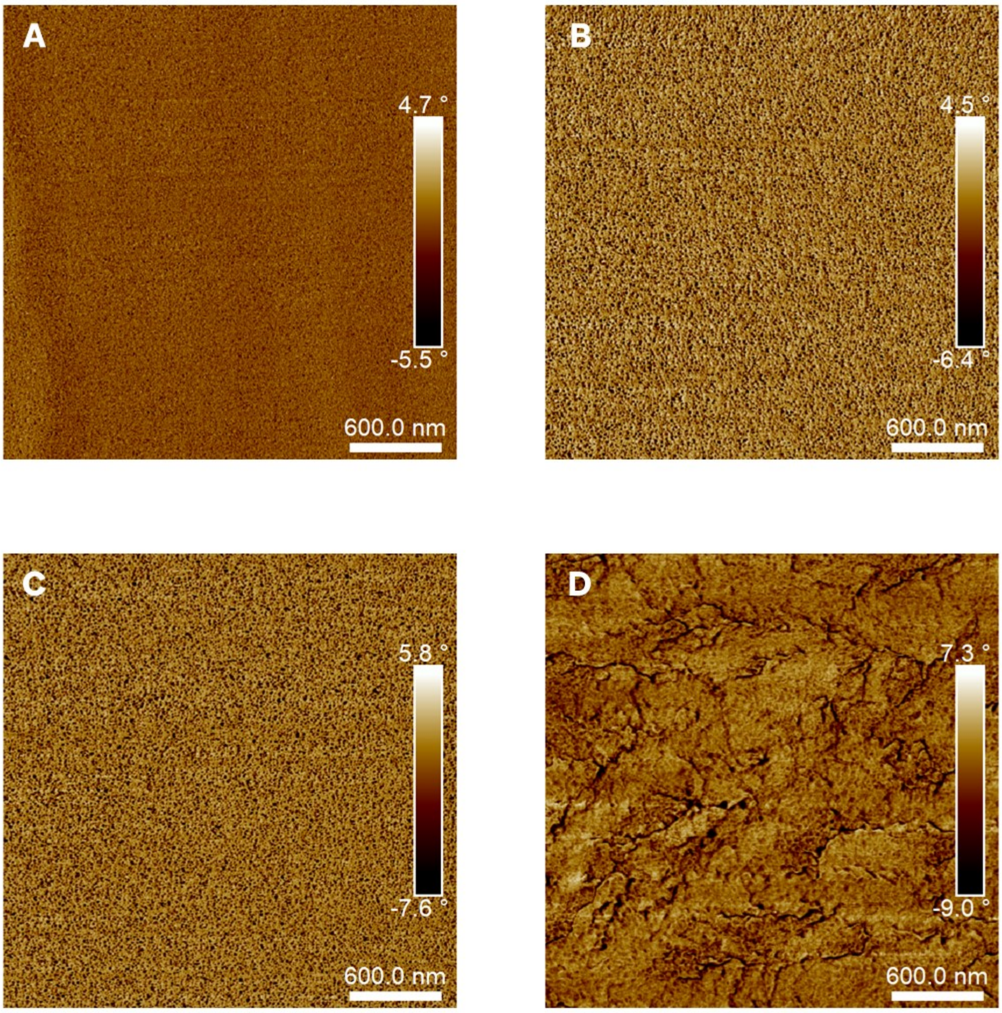

Figure 4.7: 3 μm scan size AFM phase images of (A) neat DGEVA/DDM and DGEVA/DDM-BCP systems with (B) 10 wt%,(C) 20 wt%, (D) 40 wt%, of PEO-PPO-PEO

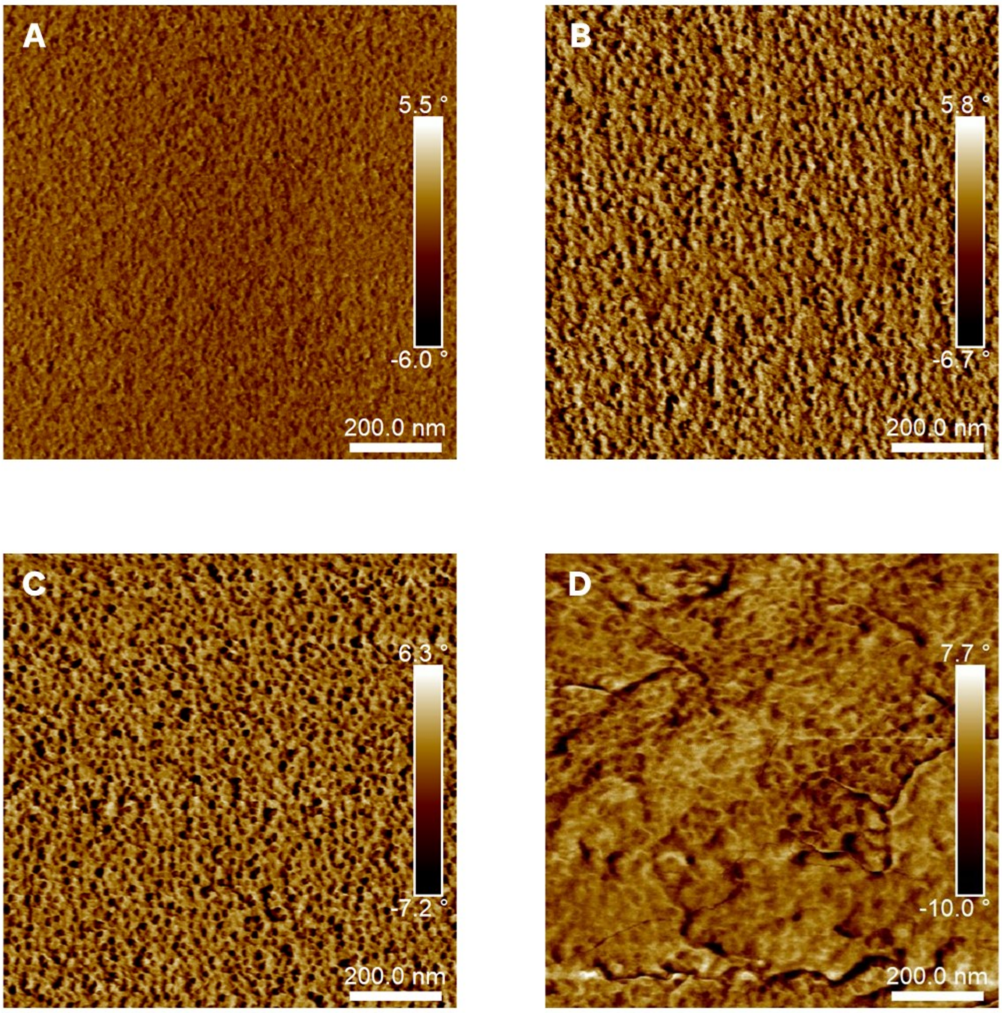

Figure 4.8: 1 μm scan size AFM phase images of (A) neat DGEVA/DDM and DGEVA/DDM-BCP systems with (B) 10 wt%,(C) 20 wt%, (D) 40 wt%, of PEO-PPO-PEO

4.1.5 Swelling Index and Gel Content measurements

The extent of the crosslinking was studied with swelling index and gel content measurements. The neat epoxy sample does not undergo swelling. The addition of 10% of BCP does not affect the swelling of the material. With higher amounts of PEO-PPO-PEO triblock copolymer the SI increases proportionally with the BCP content, from 11.7% for the DGEVA/DDM-BCP20 system to 23.4% for the DGEVA/DDM-BCP40 one.

The gel content of the systems up to 20% is not affected by the BCP content, showing high conversion rate of the amine-epoxy reaction and an excellent network connectivity. It's important to highlight that the GC for these systems is higher than the amount of epoxy resin present. This can be justified knowing that a nanostructure is obtained, which prevents the PEO-PPO-PEO triblock copolymer to be solved in the THF. *Razquin et al.*[34] reported a similar behaviour for a photocured DGEBA epoxy resin blended with 50 wt% polycaprolactone (PCL). The epoxy resin prevented a fraction of the PCL to be solved and the GC resulted around 85% for the studied systems.

For the DGEVA/DDM-BCP40 system the GC decreases to 73%, still higher than the amount of epoxy resin in the system. In this case, as already said, the high amount of BCP disrupts the nanostructuring of the system forming crystalline domains of PEO-PPO-PEO triblock copolymer. The network has a lower connectivity and it allows a fraction of the copolymer to be solved in THF.

Table 4.3: Swelling Index and Gel Content values of the neat DGEVA/DDM system and DGEVA/DDM-BCP ones

	SI (%)	GC (%)
DGEVA/DDM	0	99
DGEVA/DDM-BCP10	0	99
DGEVA/DDM-BCP20	11.7	100
DGEVA/DDM-BCP40	23.4	73

4.1.6 Contact Angle measurements

The hydrophilic nature of DGEVA/DDM-BCP blends and its dependence on the BCP content were analysed by contact angle measurements. The results are shown in Table 4.4. The contact angle decreases continuously with the amount of BCP in the system, varying from 76.84° for the DGEVA/DDM system to 40.53° for the DGEVA/DDM-BCP40 one. At the same time, for these systems, the surface energy increases from 27.1 to 55.8 mN/m, respectively. This could be explained by the presence at the surface of PEO blocks of the BCP and their hydrophilic nature. A similar behaviour is reported in the literature for a system of PEO-PPO-PEO mixed with DGEBA resin; in that case the neat epoxy presented a contact angle of 83.4° which decreased to 29.5 with a 50 wt% of PEO-PPO-PEO copolymer[28].

The increase of the hydrophilic nature of the blends can be observed in Figure 4.9. For the DGEVA/DDM it is possible to observe a sphere-like drop in the surface of the sample, while the samples with BCP tend to have a less spherical profile and lower height. The DGEVA/DDM-BCP40 system is the one with the lowest contact angle and the lowest drop height.

Table 4.4: Water contact angle and surface free energy values of the cured DGEVA/DDM-BCP systems

	Contact angle (°)	γ_{SV} (mN/m)
DGEVA/DDM	76.84 ± 0.67	27.1
DGEVA/DDM-BCP10	72.40 ± 0.26	30.5
DGEVA/DDM-BCP20	69.96 ± 0.26	32.4
DGEVA/DDM-BCP40	40.53 ± 1.32	55.8

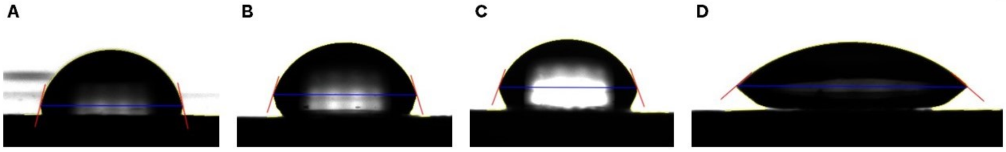

Figure 4.9: Images of a water droplet in contact with A) neat epoxy, B) 10 wt % BCP/epoxy, C) 20 wt % BCP/epoxy, D) 40 wt % BCP/epoxy systems.

4.1.7 Three-point flexural test

The mechanical properties of all the systems were studied with a three-point flexural test without notch. The complete results are shown in Table 4.5. The Force-Displacement curves are reported in the supplementary material, along with the complete results of the tests.

The stress-deformation curves, shown in Figure 4.10, present an elastic region limited to lower stress with increasing amount of BCP in the systems. The addition of PEO-PPO-PEO triblock copolymer reduces the rigidity of the blends: the stress required to reach a certain deformation decreases proportionally with the amount of BCP present in the system. As shown in Figure 4.11, the flexural modulus of the neat epoxy resin is 3.94 GPa. The results are in accordance with similar systems found in the literature: the flexural modulus of a DGEBA/DDM system is 3.19 GPa[35]. *Dai et al.*[36] reported a similar biobased epoxy resin from diglycidyl ether of genistein (DGEG) cured with DDM which presented a flexural modulus of 2.94 GPa.

The addition of BCP in the resin results in a proportional reduction of the flexural modulus with the increase of BCP content, from 2.93 GPa for the DGEVA/DDM-BPC10 system to 0.38 GPa for the DGEVA/DDM-BCP40 one, one order of magnitude lower with respect to the DGEVA/DDM sample. The same behaviour is seen for the flexural strength,shown in Figure 4.12, which decreases from 142.14 MPa for the DGEVA/DDM system to 2.36 MPa of the DGEVA/DDM-BCP40 one.

This fact could be attributed to a plasticization effect of PEO-PPO-PEO, due to the partial miscibility between the epoxy and the PEO blocks in the BCP. In addition, with higher amount of BCP there's also a decrease in the crosslinking density of the systems, which could be another factor in the reduction of the mechanical properties. Other authors have reported similar behaviours for epoxy systems and BCP blends: *Builes et al.*[37] studied an unsaturated polyester resin nanostructured by PEO-PPO-PEO; they reported a drop of one order of magnitude from the neat resin to the system with 50 wt% of BCP. *Cano et al.*[28] reported a decrease in the flexural modulus of DGEBA epoxy resin nanostructured with PEO-PPO-PEO up to a content of 25 wt%.

Table 4.5: Mechanical properties of DGEVA/DDM-BCP systems with BCP content from 0 to 40 wt%

	E (GPa)	σ_f (MPa)
DGEVA/DDM	3.94 ± 0.11	124.14 ± 5.00
DGEVA/DDM-BCP10	2.93 ± 0.03	102.48 ± 1.07
DGEVA/DDM-BCP20	1.92 ± 0.08	66.99 ± 3.75
DGEVA/DDM-BCP40	0.38 ± 0.05	2.36 ± 0.31

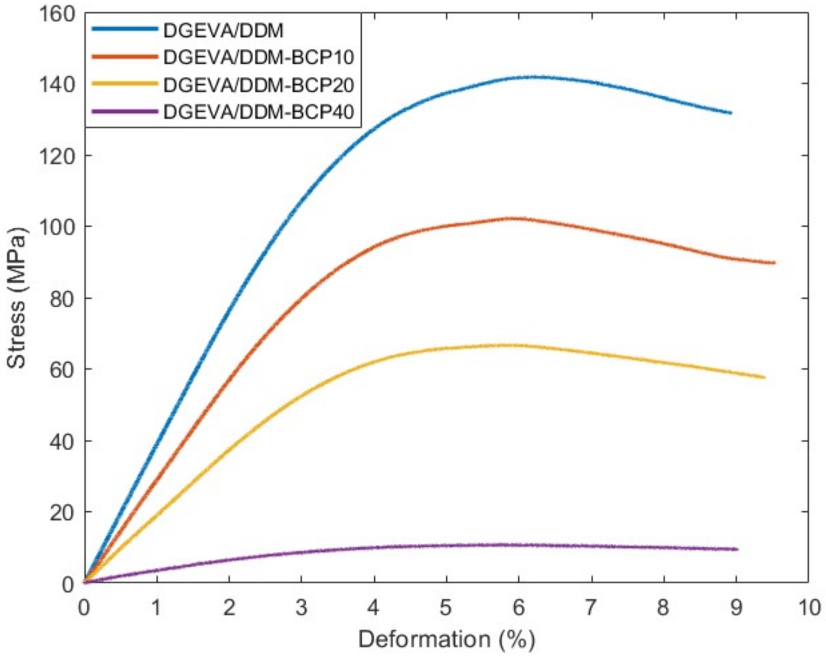

Figure 4.10: Stress-Deformation curves of DGEVA/DDM-BCP bulk systems with BCP content from 0 to 40 wt%

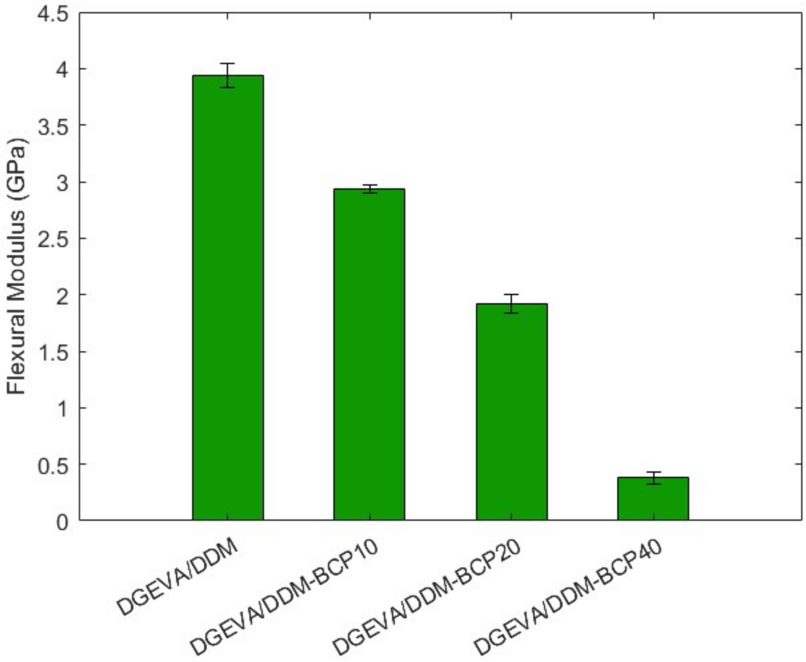

Figure 4.11: Flexural modulus of DGEVA/DDM-BCP bulk systems with BCP content from 0 to 40 wt%

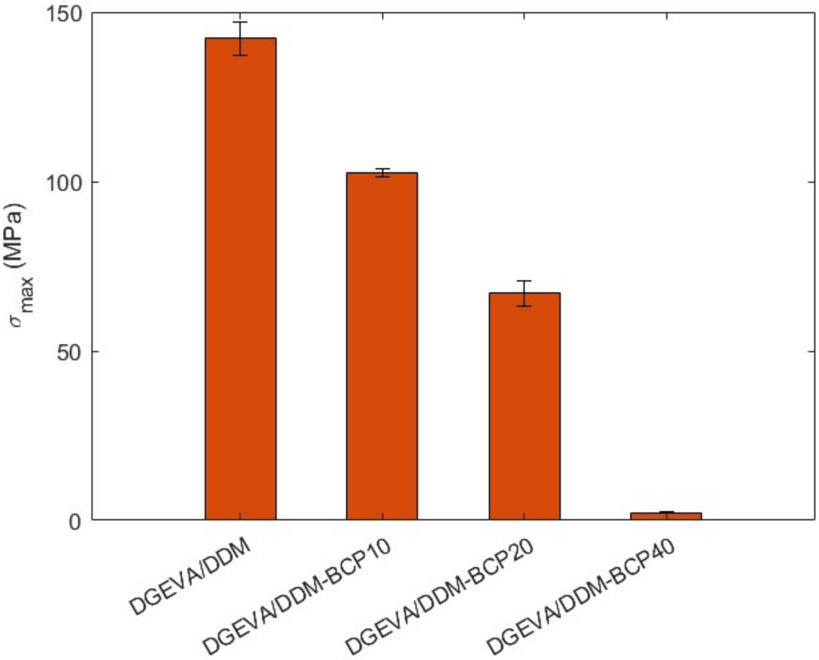

Figure 4.12: Maximum stress of DGEVA/DDM-BCP bulk systems with BCP content from 0 to 40 wt%

5. Preliminary work on biobased curing agent

5.1 Fourier-Transform Infrared Spectroscopy

In Figure 5.1 the spectrum of pristine DGEVA is compared with the one of the modified resin. The pristine DGEVA sample presents the characteristic peak at 910 cm^{-1} related to the epoxy rings. In the DHAVA sample this peak does not appear, proving of a successful opening of the oxirane rings.

The pristine DGEVA resin also presents a broad peak centered at 3433 cm^{-1} which, as already mentioned, can be related to the stretching of the -OH groups present in the sample due to retained humidity. In the modified system this broad peak undergoes a redshift to 3334 cm^{-1}. In addition, it's possible to identify two small peaks at 3302 and 3363 cm^{-1}, related to the asymmetric and symmetric stretching of -NH_2 in the amine moieties of the molecule, respectively[38].

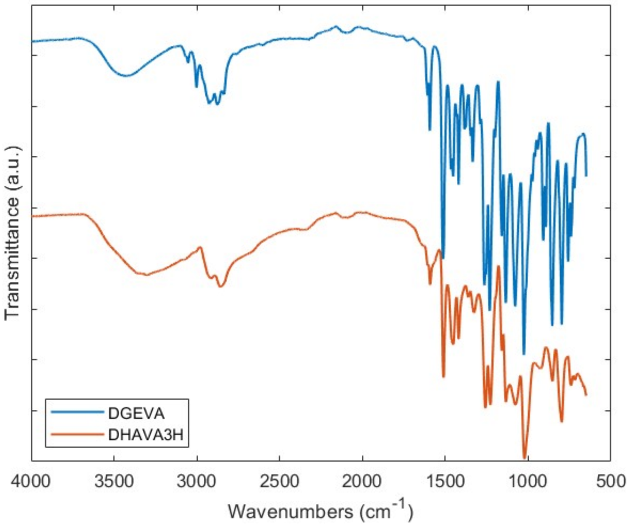

Figure 5.1: FTIR spectra of pristine DGEVA and DHAVA

5.2 ^{1}H-Nuclear Magnetic Resonance (^{1}H-NMR)

The chemical structure of the molecule obtained after the modification of DGEVA was investigated with ^{1}H-NMR analysis. The spectrum, shown in Figure 5.2, presents two signals at 2.72 and 2.87 ppm, which are related to α-CH_2 (14 and 1) bonded with the amines. In the region of lower chemical displacements it is possible to observe the signals of α-CH bonded with hydroxyl groups (13 at δ=3.97 ppm and 2 at δ=4.10 ppm) and with α-O-CH_2 (12 at δ=3.46 ppm). In addition, the typical signal of the singlet, associated with the metoxy group α-O-CH_3 can be identified at 3.84 ppm. Finally, the signals related to the aromatic ring (at 6.87, 6.90 and 6.97 ppm) confirm the amination of the DGEVA resin.

The molecule obtained through this synthesis method is confirmed to be the dihydroxyaminopropane of vanillyl alcohol (DHAVA), its chemical structure is also shown in Figure 5.2.

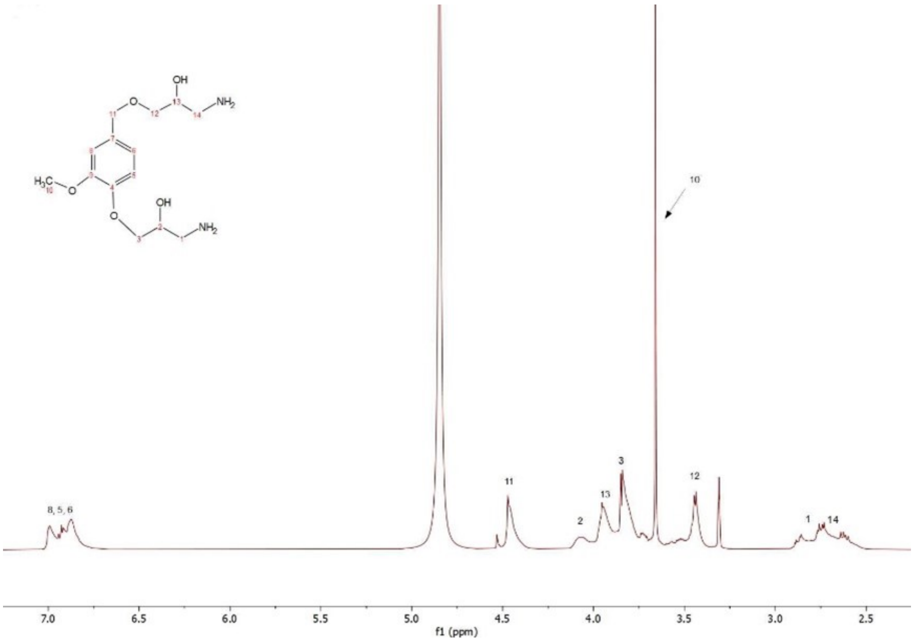

Figure 5.2: ^{1}H-NMR spectrum of the modified DGEVA

6. Future Work

In the pursuit of obtaining a fully biobased epoxy system, the synthesis of a biobased curing agent is essential. Future work should first optimize the synthesis procedure of DHAVA and then evaluate the performance of DHAVA and its amine-epoxy curing reaction. In the study of the curing process, an analysis of the optimal ratio between DGEVA and DHAVA should be carried out first. Then, the curing cycle of a DGEVA/DHAVA system should be studied and optimized.

Once DGEVA/DHAVA systems are successfully obtained, the possibility of nanostructuring should be explored, as was done with the DGEVA/DDM systems.

Additionally, the research should focus on expanding the possible applications of these systems. The potential of exploiting these nanostructured materials not only as bulk materials but also as thin films should be explored. One potential application is to use it as a coating, so both the processing of the coating and its specific characteristics as a coating will have to be analyzed.

7. Conclusions

Nanostructured epoxy resin systems modified with several contents of PEO-PPO-PEO triblock copolymer were successfully prepared. The addition of BCP into DGEVA epoxy resin resulted to be an effective method to obtain nanophase separation induced by self-assembly. The following conclusions can be drawn out from this work:

- The curing temperature was set at 120°C, from previous work[27]: this temperature allowed to fully cure all the systems regardless of the BCP content, while giving enough time to the PEO-PPO-PEO triblock copolymer to self-assemble into nanodomains.

- As was confirmed by AFM, the cured systems showed well nanostructured morphologies up to 20 wt%, with the morphology being dependent on the BCP content; The DGEVA/DDM-BCP10 system showed a spherical structure, which shifted to an hexagonally packed cylinder morphology for the DGEVA/DDM-BCP20 one. The DGEVA/DDM-BCP40 system showed also a level of nanostructuring, but the high amount of BCP caused the formation of crystalline regions, which disrupted the nanophase separation.

- The addition of BCP in the epoxy also caused a decrease in the T_g of the systems, which was found to be proportional to the BCP amount. Additionally, the DGEVA/DDM-BCP40 system presented three distinct T_g, caused by the more complex structure of the system: they were attributed to a phase of neat PEO-PPO-PEO, a PEO phase with DGEVA and a PEO rich DGEVA phase.

- The nanostructured thermosets showed a high network connectivity as was confirmed by the gel contents: the nanophase separation prevented the BCP in the systems to be solved in THF. In addition, the hydrophilicity of the systems was proved to be dependent on the BPC content and it increased proportionally.

- The mechanical properties were highly influenced by the content of BCP. The neat DGEVA/DDM system showed a flexural modulus of 3.94 GPa. This property dropped of an order of magnitude with a BCP content of 40 %, as the DGEVA/DDM-BCP40 system showed a modulus of 0.38 GPa.

- Finally, starting from the DGEVA resin, a DHAVA curing agent was successfully synthesised, as confirmed confirmed by ^{1}H-NMR analysis .

8. Bibliography

[1] Lucie Pierau et al. *Bio-sourced monomers and cationic photopolymerization–The green combination towards eco-friendly and non-toxic materials.* Apr. 2022. DOI: `10.1016/j.progpolymsci.2022.101517`.

[2] Hanna Faltynowicz, Marek Kułażynski, and Sidney H. Goodman. "Epoxies". In: *Handbook of Thermoset Plastics.* Elsevier, Jan. 2021, pp. 175–229. ISBN: 9780128216323. DOI: `10.1016/B978-0-12-821632-3.00014-2`.

[3] Clayton A May. *Epoxy Resins: Chemistry and Technology.* Second Edition. Routledge, 1988. ISBN: 978-0824776909.

[4] Ha Q. Pham and Maurice J. Marks. "Epoxy Resins". In: *Encyclopedia of Polymer Science and Technology* (July 2004). DOI: `10.1002/0471440264.pst119`.

[5] Jaworski C. Capricho, Bronwyn Fox, and Nishar Hameed. *Multifunctionality in Epoxy Resins.* Jan. 2020. DOI: `10.1080/15583724.2019.1650063`.

[6] Hanna Dodiuk and Sidney H. Goodman. "Introduction". In: *Handbook of Thermoset Plastics.* Elsevier Inc., 2014, pp. 1–12. ISBN: 9781455731077. DOI: `10.1016/B978-1-4557-3107-7.00001-4`.

[7] Ayman M. Atta, Nevin O. Shaker, and Notaila E. Nasser. "Synthesis of bisphenol a novolac epoxy resins for coating applications". In: *Journal of Applied Polymer Science* 107 (1 Jan. 2008), pp. 347–354. ISSN: 00218995. DOI: `10.1002/app.26981`.

[8] Fan Long Jin, Xiang Li, and Soo Jin Park. "Synthesis and application of epoxy resins: A review". In: *Journal of Industrial and Engineering Chemistry* 29 (Sept. 2015), pp. 1–11. ISSN: 22345957. DOI: `10.1016/j.jiec.2015.03.026`.

[9] Sudheer Kumar et al. "Synthesis and characterization of petroleum and biobased epoxy resins: a review". In: *Polymer International* 67 (7 July 2018), pp. 815–839. ISSN: 10970126. DOI: `10.1002/pi.5575`.

[10] Weiwei Zhao et al. *Bio-Based Thermosetting Resins: From Molecular Engineering to Intrinsically Multifunctional Customization.* Sept. 2024. DOI: `10.1002/adma.202311242`.

[11] Yuan Zhang et al. *From renewable biomass to bio-based epoxy monomers and bio-based epoxy curing agents: Synthesis and performance.* Nov. 2024. DOI: `10.1016/j.polymdegradstab.2024.110988`.

[12] Maxence Fache, Bernard Boutevin, and Sylvain Caillol. “Vanillin Production from Lignin and Its Use as a Renewable Chemical”. In: *ACS Sustainable Chemistry and Engineering* 4 (1 Jan. 2016), pp. 35–46. ISSN: 21680485. DOI: `10.1021/acssuschemeng.5b01344`.

[13] Xinyu Lu et al. “Selective Catalytic Transfer Hydrogenation of Lignin to Alkyl Guaiacols Over NiMo/Al-MCM-41”. In: *ChemSusChem* 15 (7 Apr. 2022). ISSN: 1864564X. DOI: `10.1002/cssc.202200099`.

[14] Chinnappan Baskar, Shikha Baskar, and Ranjit S. Dhillon. *Biomass conversion: The interface of biotechnology, chemistry and materials science.* Vol. 9783642284182. Springer-Verlag Berlin Heidelberg, Jan. 2012, pp. 1–465. ISBN: 9783642284182. DOI: `10.1007/978-3-642-28418-2`.

[15] Xinyu Lu and Xiaoli Gu. *A review on lignin-based epoxy resins: Lignin effects on their synthesis and properties.* Feb. 2023. DOI: `10.1016/j.ijbiomac.2022.12.322`.

[16] Sylvain Caillol et al. “Eugenol, a developing asset in biobased epoxy resins”. In: 223 (2021). DOI: `10.1016/j.polymer.2021.123663Ãŕ`.

[17] Jianglei Qin et al. “Use of eugenol and rosin as feedstocks for biobased epoxy resins and study of curing and performance properties”. In: *Polymer International* 63 (4 2014), pp. 760–765. ISSN: 10970126. DOI: `10.1002/pi.4588`.

[18] Shou Zhao and Mahdi M. Abu-Omar. “Biobased epoxy nanocomposites derived from lignin-based monomers”. In: *Biomacromolecules* 16 (7 July 2015), pp. 2025–2031. ISSN: 15264602. DOI: `10.1021/acs.biomac.5b00670`.

[19] Etienne Savonnet et al. “Divanillin-Based Aromatic Amines: Synthesis and Use as Curing Agents for Fully Vanillin-Based Epoxy Thermosets”. In: *Frontiers in Chemistry* 7 (Sept. 2019). ISSN: 22962646. DOI: `10.3389/fchem.2019.00606`.

[20] Nour Mattar et al. “Resorcinol-Based Epoxy Resins Hardened with Limonene and Eugenol Derivatives: From the Synthesis of Renewable Diamines to the Mechanical Properties of Biobased Thermosets”. In: *ACS Sustainable Chemistry and Engineering* 8 (34 Aug. 2020), pp. 13064–13075. ISSN: 21680485. DOI: `10.1021/acssuschemeng.0c04780`.

[21] Jia Li Huang et al. “Cardanol-derived anhydride cross-linked epoxy thermosets with intrinsic anti-flammability, toughness and shape memory effect”. In: *Chemical Engineering Journal* 450 (Dec. 2022). ISSN: 13858947. DOI: `10.1016/j.cej.2022.137906`.

[22] Goerg H.. Michler and F. J.. Balta-Calleja. *Nano- and micromechanics of polymers : structure modification and improvement of properties*. Hanser, 2012, p. 566. ISBN: 9783446427679.

[23] Galder. Kortaberria and Agnieszka. Tercjak. “Block copolymer nanocomposites”. In: Pan Stanford Publishing, 2017, p. 345. ISBN: 9789814669542.

[24] Galder Kortaberri. “Nanostructured Morphologies by Self-Assembly of Diblock Copolymers: A Review”. In: *Molecular Self-assembly in Nanoscience and Nanotechnology*. InTech, May 2017. DOI: `10.5772/intechopen.68476`.

[25] Cian Cummins et al. “Enabling future nanomanufacturing through block copolymer self-assembly: A review”. In: *Nano Today* 35 (Dec. 2020). ISSN: 1878044X. DOI: `10.1016/j.nantod.2020.100936`.

[26] Branden A. Deyerle and Yanjie Zhang. “Effects of hofmeister anions on the aggregation behavior of PEO-PPO-PEO triblock copolymers”. In: *Langmuir* 27 (15 Aug. 2011), pp. 9203–9210. ISSN: 07437463. DOI: `10.1021/la201463g`.

[27] Irati Barandiaran et al. “Nanostructuring Biobased Epoxy Resin with PEO-PPO-PEO Block Copolymer”. In: *Polymers* 15 (5 Mar. 2023). ISSN: 20734360. DOI: `10.3390/polym15051216`.

[28] Laida Cano, Daniel H. Builes, and Agnieszka Tercjak. “Morphological and mechanical study of nanostructured epoxy systems modified with amphiphilic poly(ethylene oxide-b-propylene oxide-b-ethylene oxide)triblock copolymer”. In: *Polymer* 55 (3 Feb. 2014), pp. 738–745. ISSN: 00323861. DOI: `10.1016/j.polymer.2014.01.005`.

[29] Emilie Darroman et al. “Improved cardanol derived epoxy coatings”. In: *Progress in Organic Coatings* 91 (Feb. 2016), pp. 9–16. ISSN: 03009440. DOI: `10.1016/j.porgcoat.2015.11.012`.

[30] Anne Sophie Mora et al. “Vanillin-derived amines for bio-based thermosets”. In: *Green Chemistry* 20 (17 2018), pp. 4075–4084. ISSN: 14639270. DOI: `10.1039/c8gc02006j`.

[31] Camilla Noe et al. “Vanillin-Based Photocurable Anticorrosion Coatings Reinforced with Nanoclays”. In: *Macromolecular Materials and Engineering* (Nov. 2024). ISSN: 14392054. DOI: `10.1002/mame.202400155`.

[32] Jyotishkumar Parameswaranpillai et al. “Shape Memory Properties of Epoxy/PPO-PEO-PPO Triblock Copolymer Blends with Tunable Thermal Transitions and Mechanical Characteristics”. In: *Industrial and Engineering Chemistry Research* 56 (47 Nov. 2017), pp. 14069–14077. ISSN: 15205045. DOI: `10.1021/acs.iecr.7b03676`.

[33] Jyotishkumar Parameswaranpilla et al. “Morphology, thermo-mechanical properties and surface hydrophobicity of nanostructured epoxy thermosets modified with PEO-PPO-PEO triblock copolymer”. In: *Polymer Testing* 59 (May 2017), pp. 168–176. ISSN: 01429418. DOI: `10.1016/j.polymertesting.2017.01.029`.

[34] I. Razquin et al. “Cationically photocured epoxy/polycaprolactone materials processed by solution electrospinning, melt electrowriting and 3D printing: Morphology and shape memory properties”. In: *Polymer* 282 (Aug. 2023). ISSN: 00323861. DOI: `10.1016/j.polymer.2023.126160`.

[35] Meiying Ge et al. “Biobased epoxy resin with ultrahigh glass transition temperature over 400 °C by post-crosslinking strategy”. In: *Chemical Engineering Journal* 482 (Feb. 2024). ISSN: 13858947. DOI: `10.1016/j.cej.2024.148993`.

[36] Jinyue Dai et al. “Synthesis of bio-based fire-resistant epoxy without addition of flame retardant elements”. In: *Composites Part B: Engineering* 179 (Dec. 2019). ISSN: 13598368. DOI: `10.1016/j.compositesb.2019.107523`.

[37] Daniel H. Builes et al. “Relationship between the morphology of nanostructured unsaturated polyesters modified with PEO-b-PPO-b-PEO triblock copolymer and their optical and mechanical properties”. In: *Journal of Physical Chemistry C* 117 (7 Feb. 2013), pp. 3563–3571. ISSN: 19327447. DOI: `10.1021/jp3097617`.

[38] Xiaomin Yang et al. “A facile one-pot synthesis of versatile PEGylated platinum nanoflowers and their application in radiation therapy”. In: *International Journal of Molecular Sciences* 21 (5 Mar. 2020). ISSN: 14220067. DOI: `10.3390/ijms21051619`.

9. Supplementary material

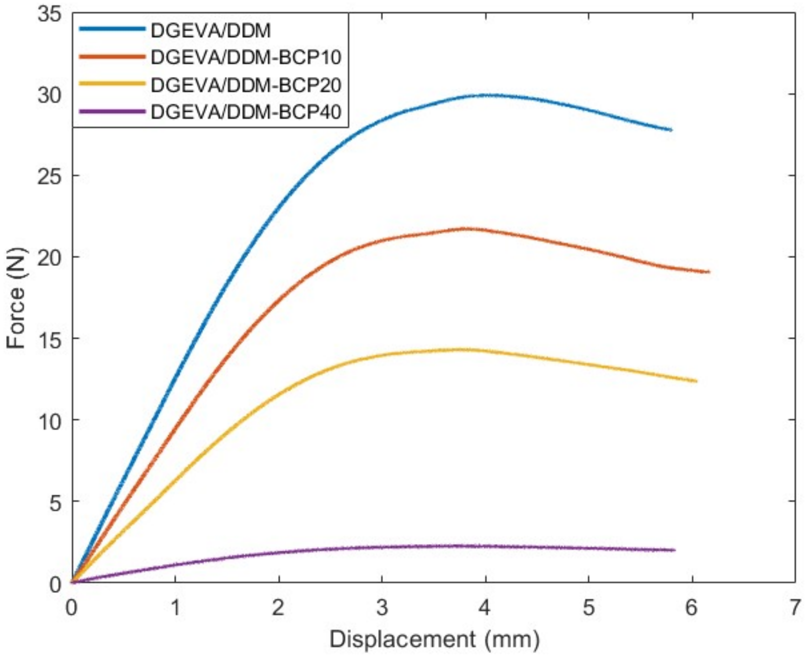

Figure 9.1: Force-Displacement curves of DGEVA/DDM-BCP bulk systems with BCP content from 0 to 40 wt%

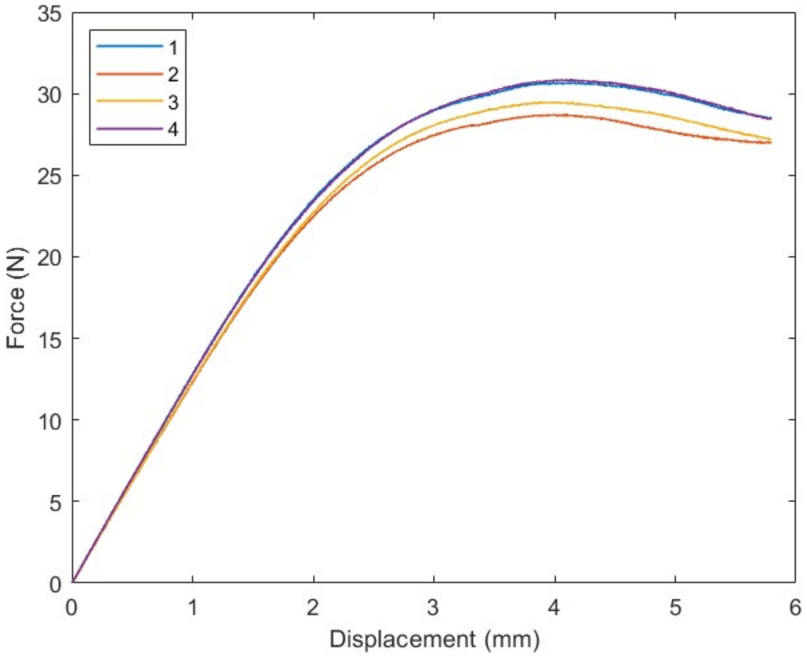

Figure 9.2: Force-Displacement curves of DGEVA/DDM neat samples

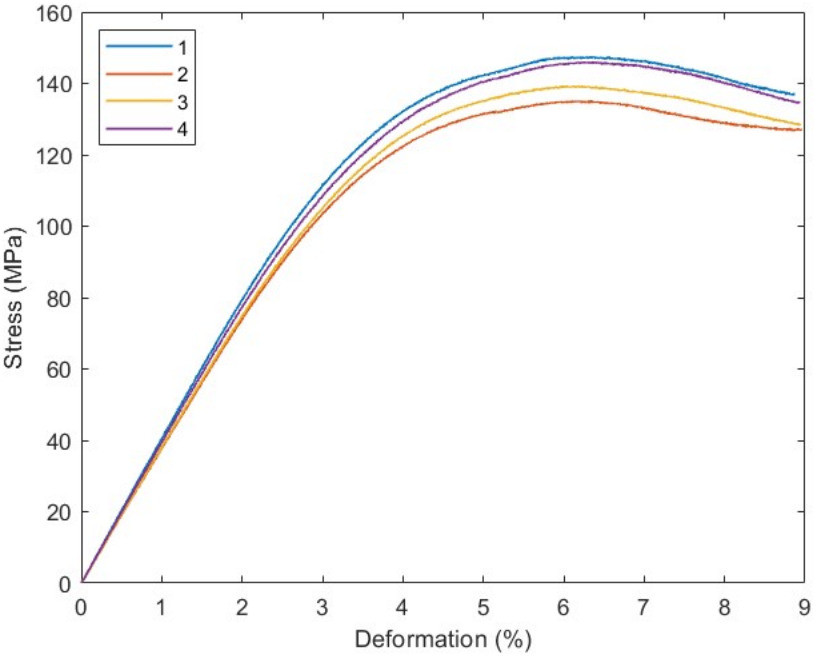

Figure 9.3: Stress-Deformation curves of DGEVA/DDM neat samples

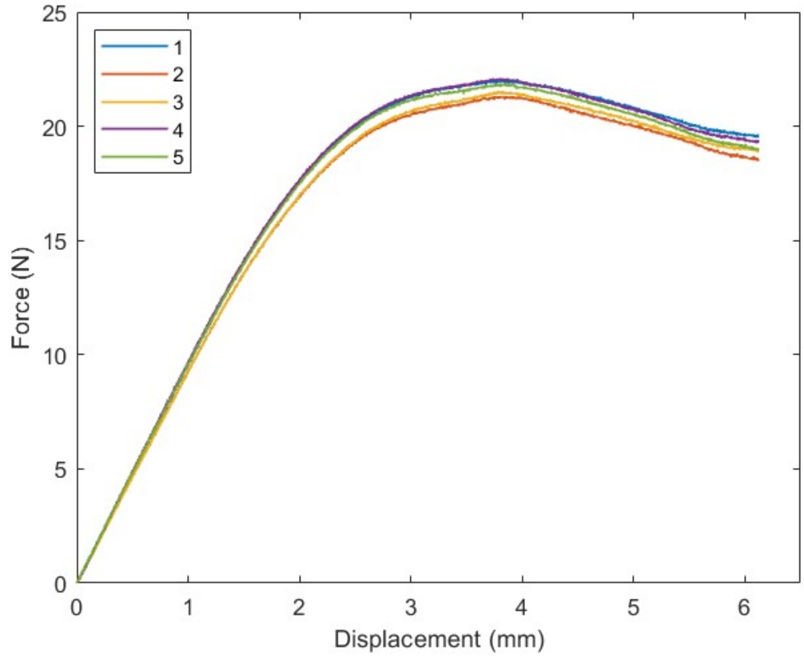

Figure 9.4: Force-Displacement curves of DGEVA/DDM-BCP10 samples

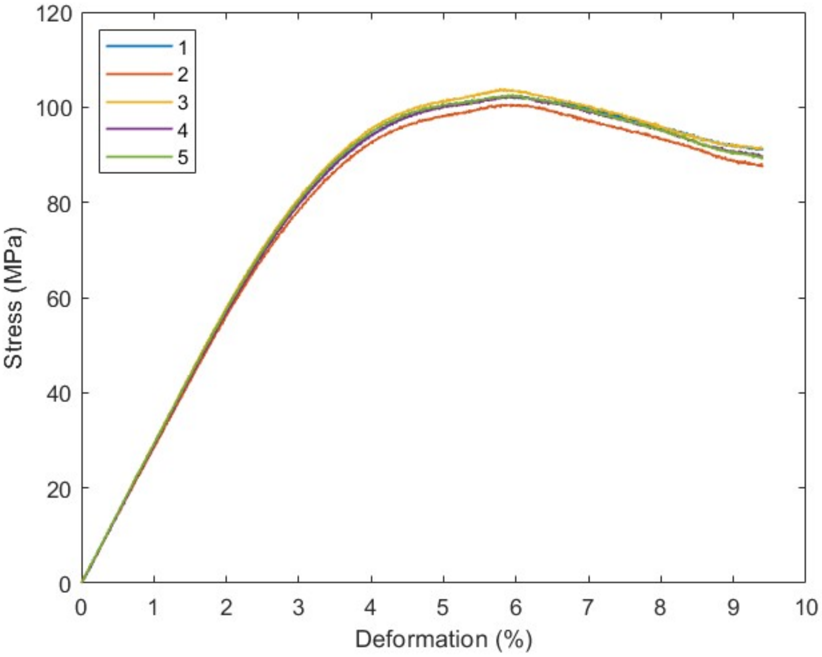

Figure 9.5: Stress-Deformation curves of DGEVA/DDM-BCP10 samples

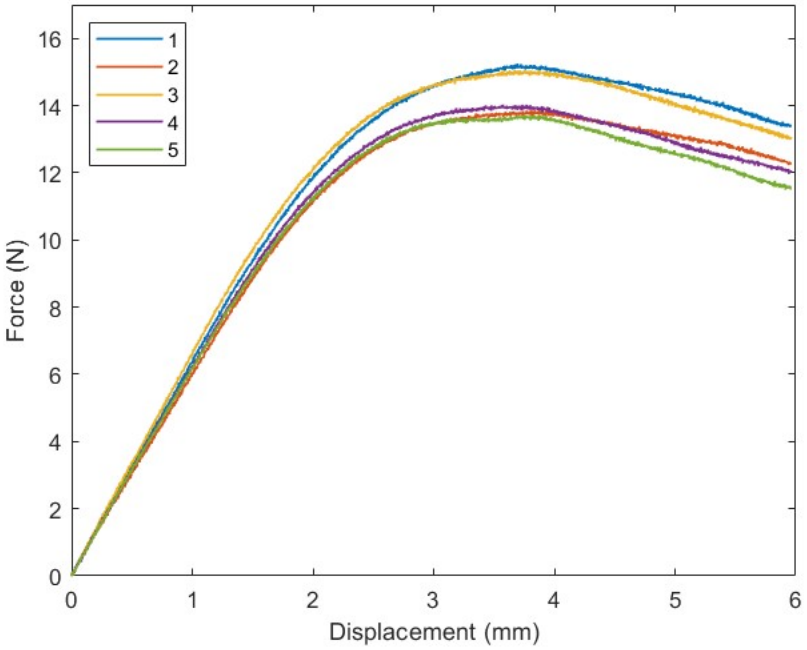

Figure 9.6: Force-Displacement curves of DGEVA/DDM-BCP20 samples

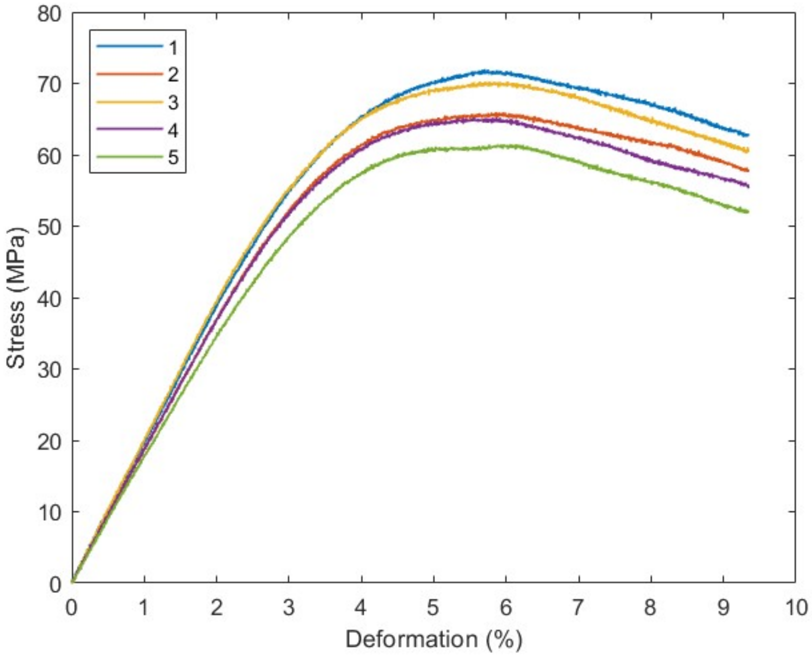

Figure 9.7: Stress-Deformation curves of DGEVA/DDM-BCP20 samples

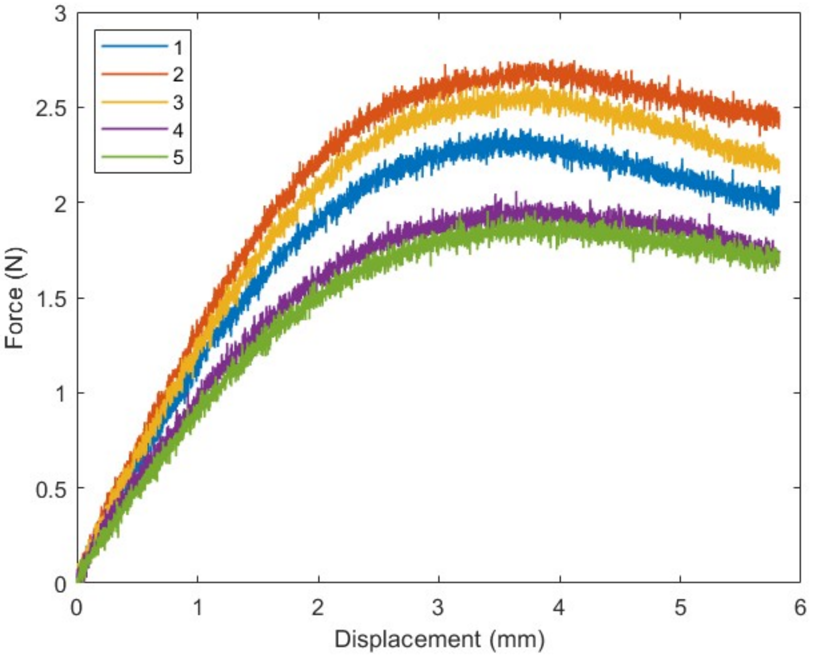

Figure 9.8: Force-Displacement curves of DGEVA/DDM-BCP40 samples

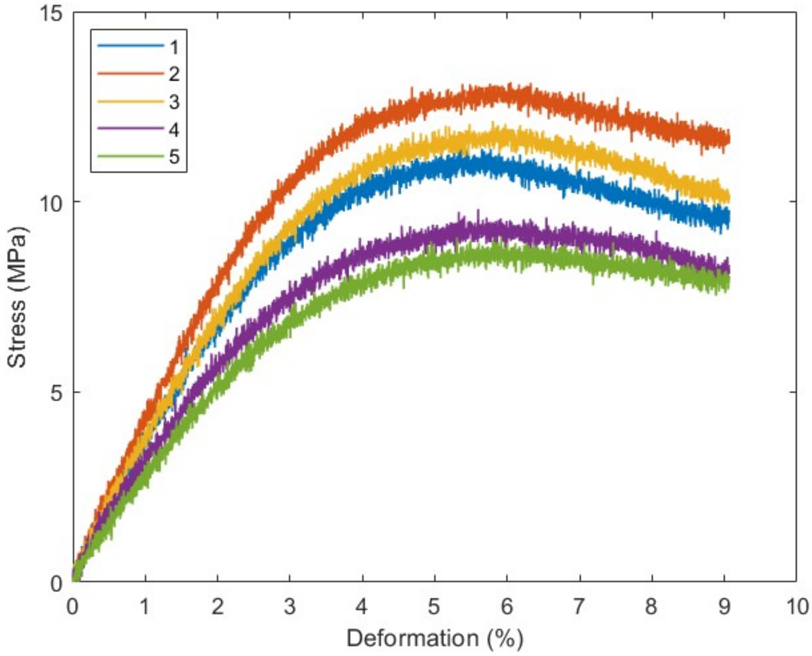

Figure 9.9: Stress-Deformation curves of DGEVA/DDM-BCP40 samples

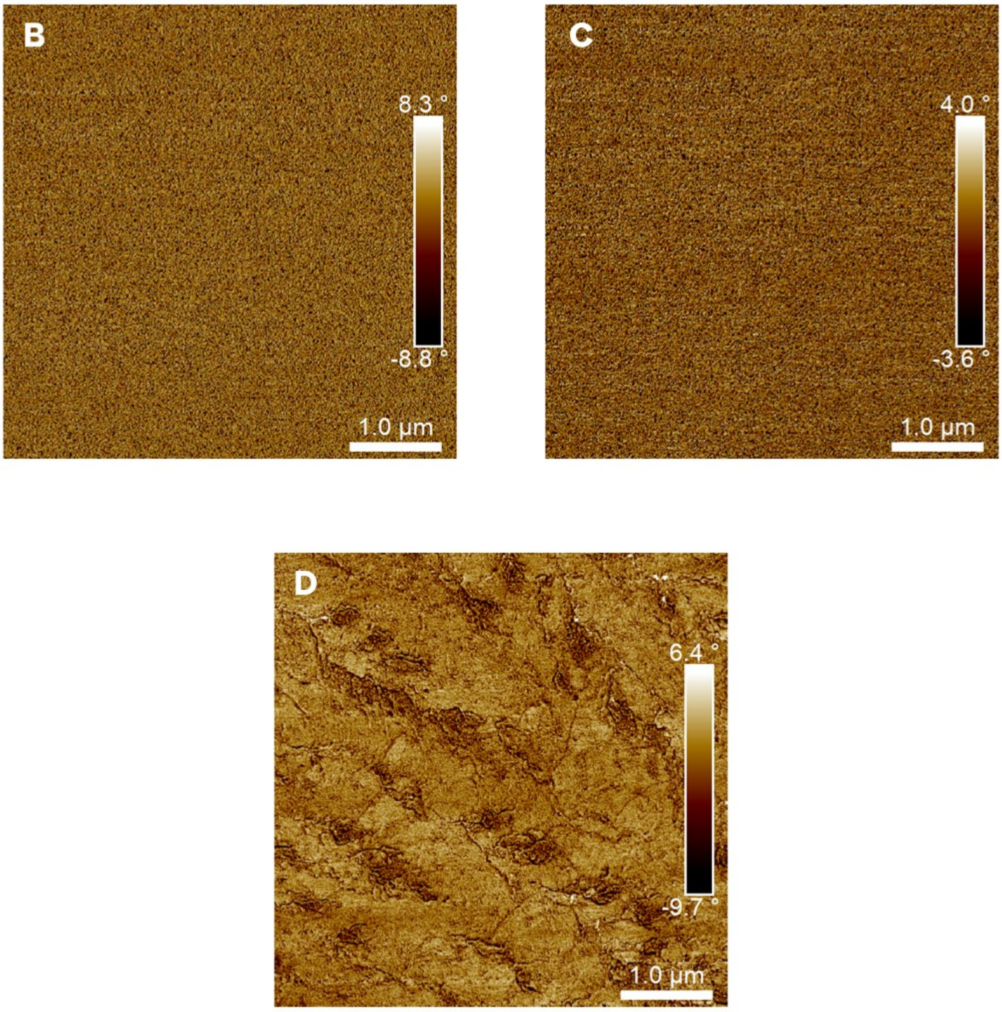

Figure 9.10: 5 μm scan size AFM phase images of DGEVA/DDM-BCP systems with (B) 10 wt%,(C) 20 wt%, (D) 40 wt%, of PEO-PPO-PEO

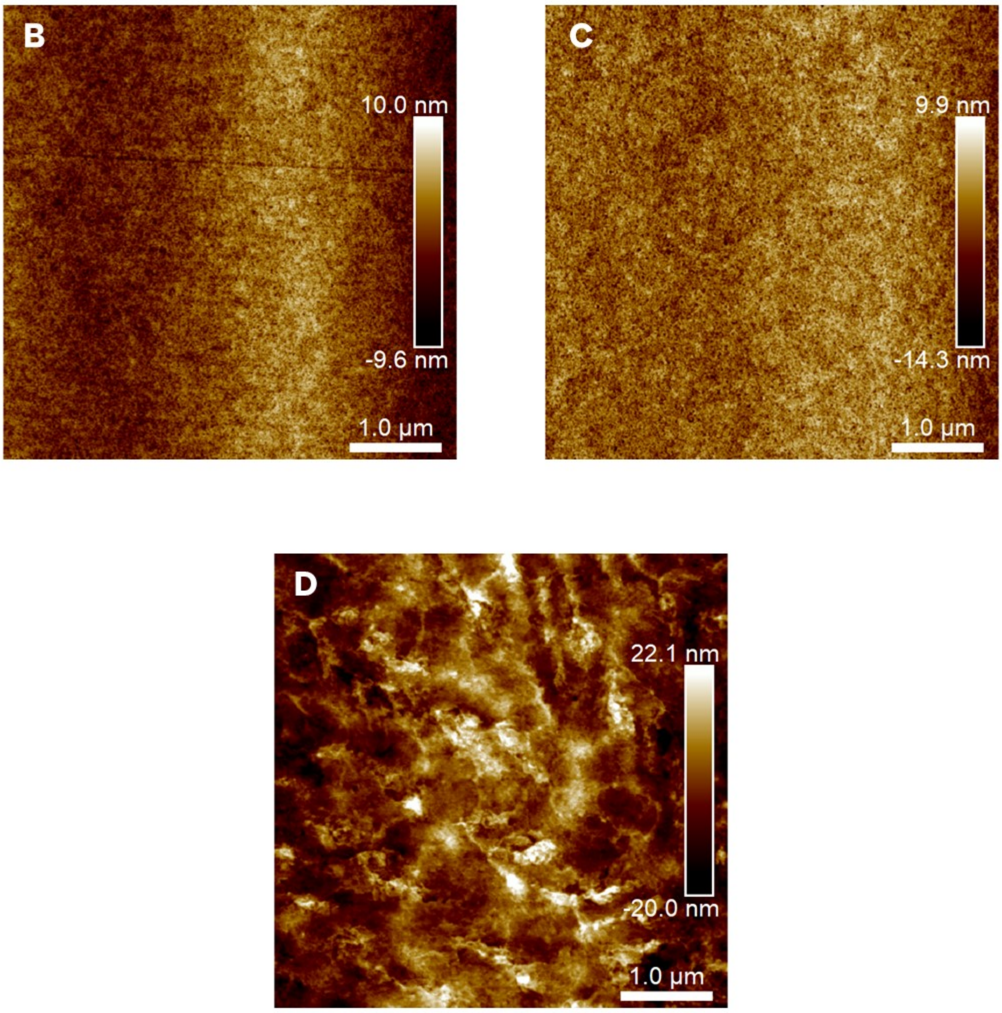

Figure 9.11: 5 μm scan size AFM height images of (A) neat DGEVA/DDM and DGEVA/DDM-BCP systems with (B) 10 wt%,(C) 20 wt%, (D) 40 wt%, of PEO-PPO-PEO

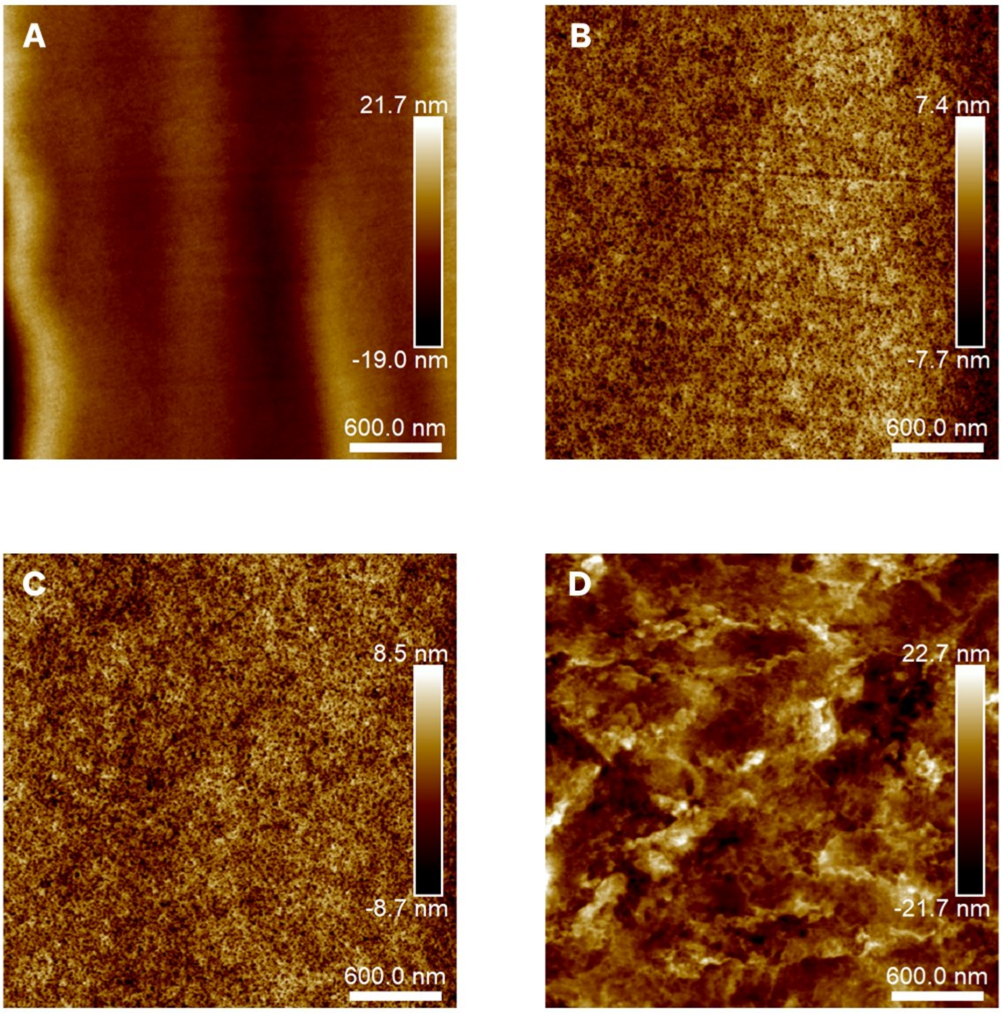

Figure 9.12: 3 μm scan size AFM height images of (A) neat DGEVA/DDM and DGEVA/DDM-BCP systems with (B) 10 wt%,(C) 20 wt%, (D) 40 wt%, of PEO-PPO-PEO

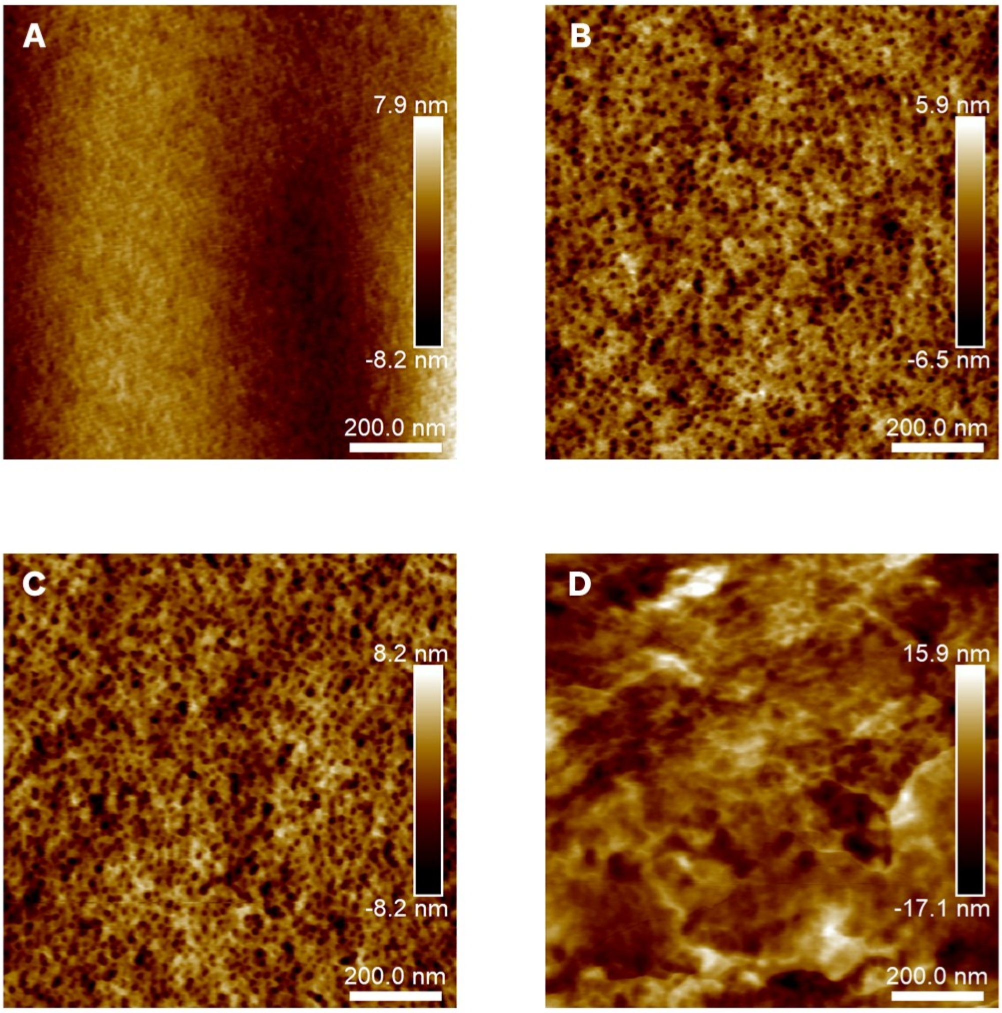

Figure 9.13: 1 μm scan size AFM height images of (A) neat DGEVA/DDM and DGEVA/DDM-BCP systems with (B) 10 wt%,(C) 20 wt%, (D) 40 wt%, of PEO-PPO-PEO